Efficient Deep Learning for Massive MIMO Channel State Estimation

Mason del Rosario

Doctoral Qualifying Examination

May 2021

Outline

Background

Feedback-based estimation of channel state information in MIMO networks.

Massive MIMO uses numerous antennas to endow transceivers with spatial diversity.

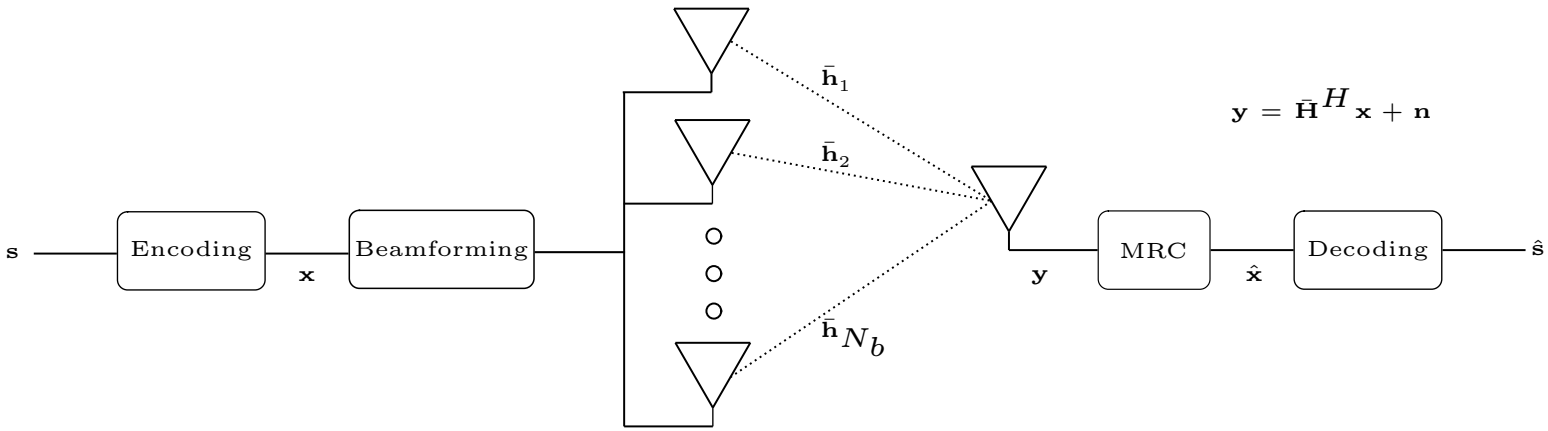

Figure: Example multi-antenna transmitter (BS, gNB) and single-antenna user equipment (UE) and relevant system values.

In OFDM, the fading coefficients between the Tx/Rx antennas constitute **Channel State Information (CSI)**, $\bar{\mathbf{H}}$. For n_T transmit antennas and n_f subcarriers,

$$\bar{\mathbf{H}} = \begin{bmatrix} h_{1,1} & h_{1,2} & \dots & h_{1,n_T} \\ h_{2,1} & h_{2,2} & \dots & h_{2,n_T} \\ \vdots & \vdots & \vdots & \vdots \\ h_{n_f,1} & h_{n_f,2} & \dots & h_{n_f,n_T} \end{bmatrix} \in \mathbb{C}^{n_f \times n_T}$$

However, transmitting $\bar{\mathbf{H}}$ is costly. Instead, generate **CSI Estimates**, $\hat{\bar{\mathbf{H}}}$, based on **compressed feedback**, $\mathbf{z}$.

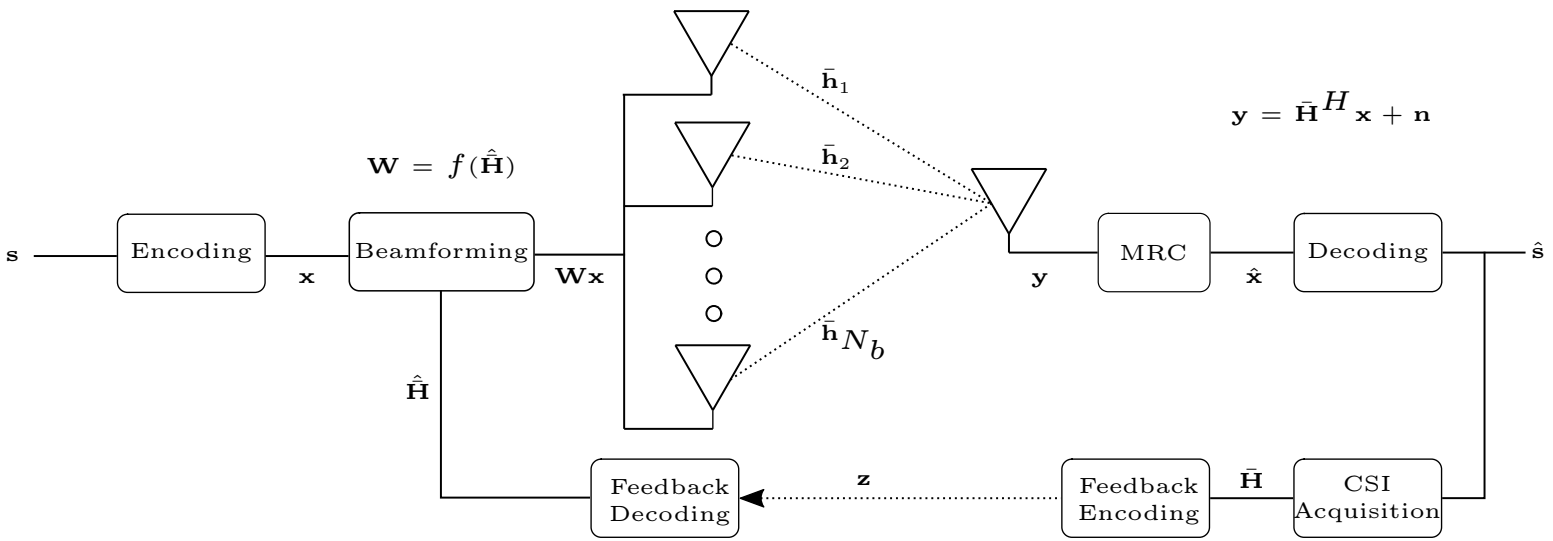

CSI Sparsity

Denote the 2D inverse FFT of $\bar{\mathbf{H}}$ as

$$\mathbf{H} = \mathbf{F}^H \bar{\mathbf{H}} \mathbf{F}.$$

While $\bar{\mathbf{H}}$ is used for beamforming, $\mathbf{H}$ is more amenable to compression.

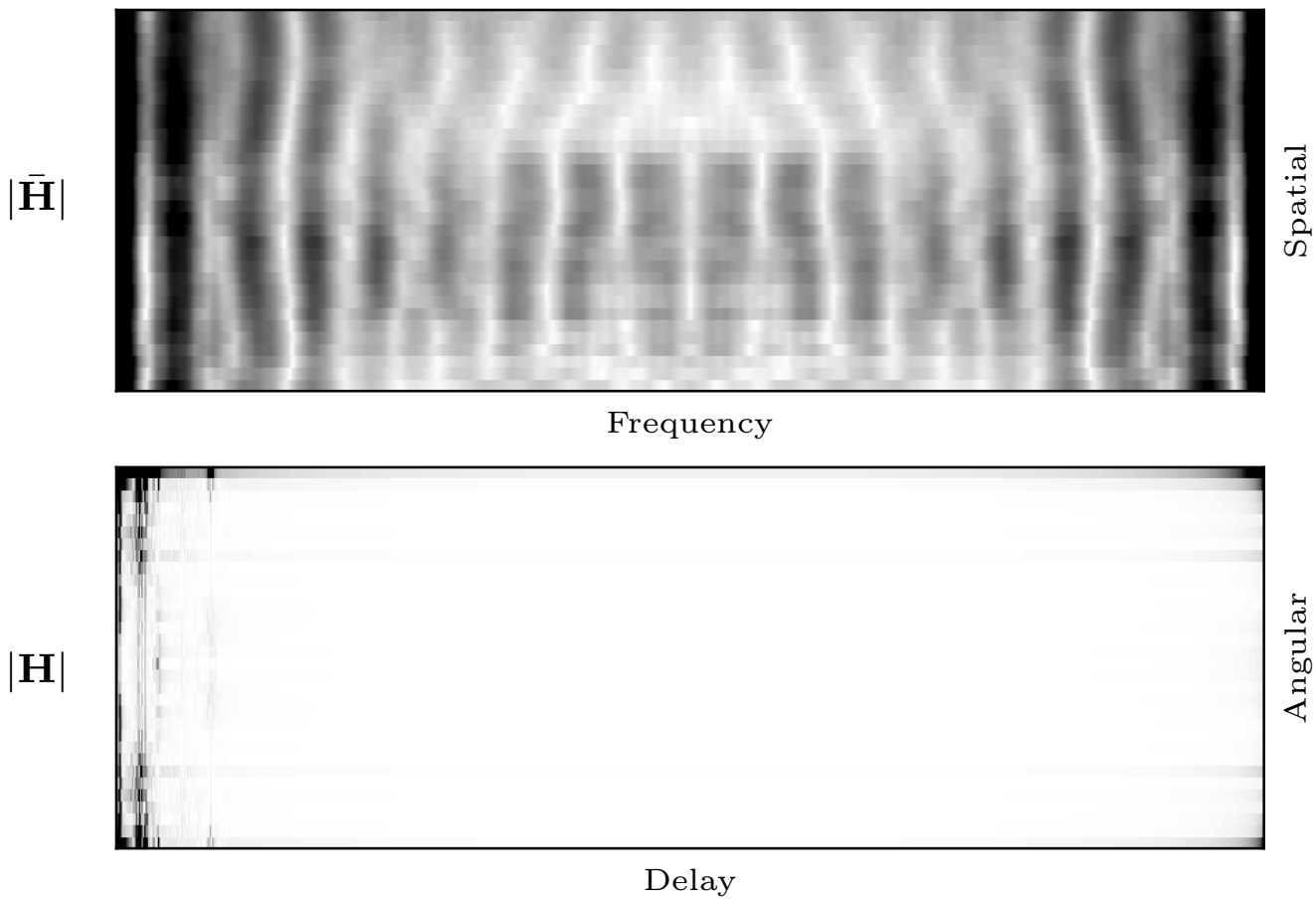

CSI Sparsity

Given the sparsity of **H** (angular-delay domain), we choose to encode a truncated **H**.

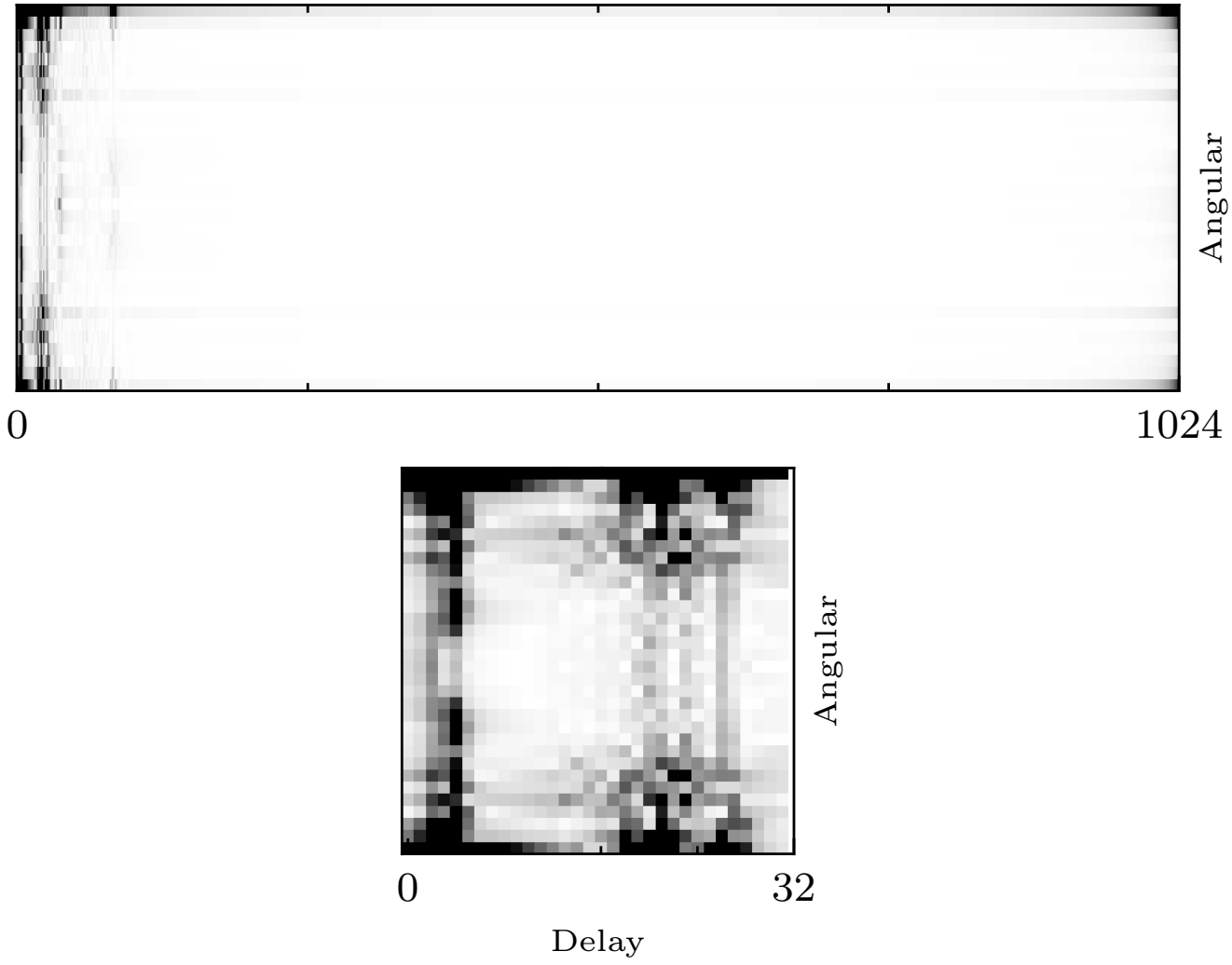

CSI Estimation Methods

1. Compressed Sensing
2. Convolutional Neural Networks

Find a low-dimensional representation of sparse data, $\mathbf{h}$, by a linear transform, $\mathbf{A}$,

$$\mathbf{y} = \mathbf{A}\mathbf{h} + \mathbf{n},$$

where $\mathbf{h}$ is a vectorized CSI measurement, $\mathbf{A}$ is the measurement matrix, and $\mathbf{n}$ is an additive noise vector.

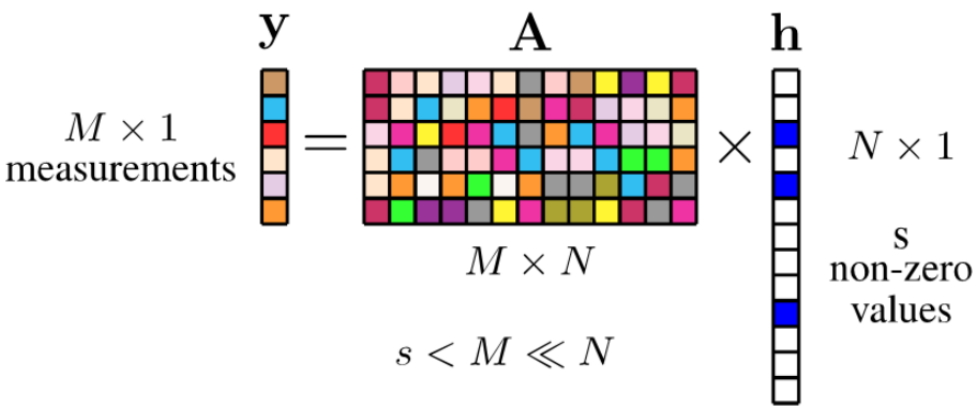

Figure: Compressed sensing via random measurement matrix $\mathbf{A}$ (from [1]).

E. Crespo Marques, N. Maciel, L. Naviner, H. Cai, and J. Yang, "A Review of Sparse Recovery Algorithms," *IEEE Access*, vol. 7, pp. 1300–1322, 2019

CS theory relies on the following assumptions:

1. The sparsity of the signal to be estimated must meet a certain level.
2. The **Restricted Isometry Criterion (RIC)** must be met. For $\delta \in [0, 1]$,

$$(1 - \delta)\|\mathbf{h}\|_F^2 \leq \|\mathbf{A}\mathbf{h}\|_F^2 \leq (1 + \delta)\|\mathbf{h}\|_F^2$$

Generally, CS approaches address two major issues:

1. The design of the measurement matrix, $\mathbf{A}$ (stochastic or deterministic).
2. The recovery of $\hat{\mathbf{h}}$ given $\mathbf{A}$ and $\mathbf{y}$ (e.g., Matching Pursuit, Orthogonal Matching Pursuit [2]).

E. C. Marques, N. Maciel, L. A. B. Naviner, H. Cai, and J. Yang, "Compressed Sensing for Wideband HF Channel Estimation," in *2018 4th International Conference on Frontiers of Signal Processing (ICFSP)*, pp. 1–5, 2018

Generally, CS approaches address two major issues:

1. The design of the measurement matrix, $\mathbf{A}$ (stochastic or deterministic).
2. The recovery of $\hat{\mathbf{h}}$ given $\mathbf{A}$ and $\mathbf{y}$ (e.g., Matching Pursuit, Orthogonal Matching Pursuit [2]).

Problem: Recovery algorithms are iterative; complexity scales with M.

E. C. Marques, N. Maciel, L. A. B. Naviner, H. Cai, and J. Yang, "Compressed Sensing for Wideband HF Channel Estimation," in *2018 4th International Conference on Frontiers of Signal Processing (ICFSP)*, pp. 1–5, 2018

Convolutional Neural Networks (CNNs)

- CNNs = state-of-the art performance in image processing
- Multiple layers of trainable linear functions followed nonlinear 'activation' functions.
- No assumptions on sparsity, RIC. Instantaneous decoding.

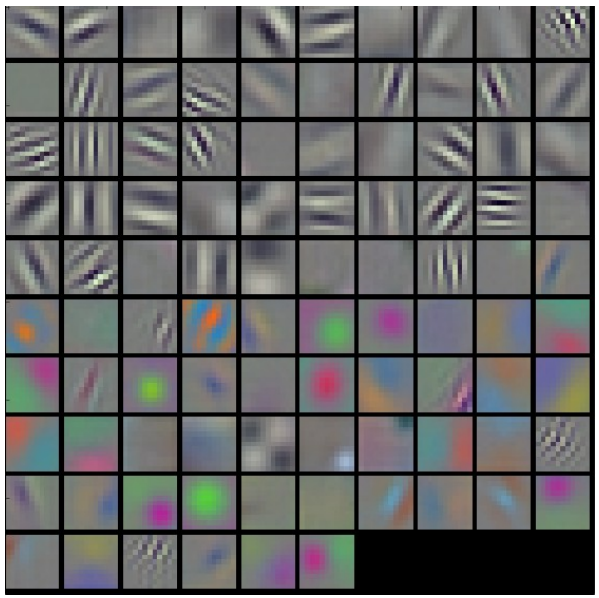

A. Karpathy, "Visualizing What ConvNets Learn," http://cs231n.github.io/understanding-cnn/. Accessed: Feb 24, 2020.

CNN Autoencoder

An autoencoder learns a latent code $\mathbf{Z}$ with **compression ratio**,

$$\text{CR} = \frac{\dim(\mathbf{Z})}{\dim(\mathbf{H})} \text{ s.t. } \dim(\mathbf{Z}) < \dim(\mathbf{H}).$$

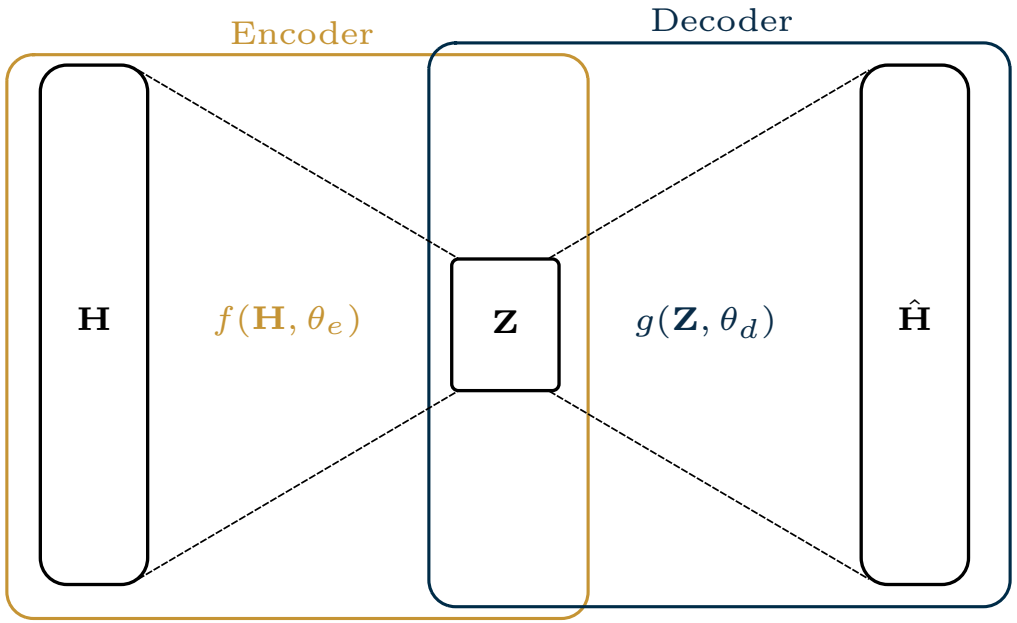

CNN Autoencoder

An autoencoder learns a latent code $\mathbf{Z}$ with **compression ratio**,

$$\text{CR} = \frac{\dim(\mathbf{Z})}{\dim(\mathbf{H})} \text{ s.t. } \dim(\mathbf{Z}) < \dim(\mathbf{H}).$$

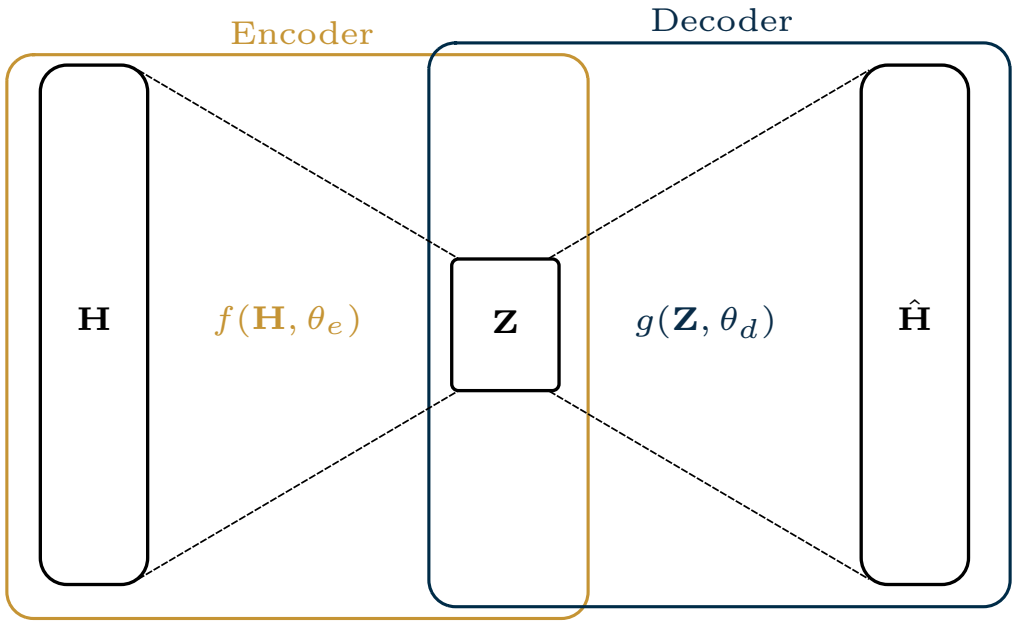

The encoder/decoder parameters θ_e, θ_d are updated via a stochastic optimizer to minimize the **mean-squared error**,

$$\underset{\theta_e, \theta_d}{\text{argmin}} \frac{1}{N} \sum_{i=1}^{N} \|\mathbf{H}_i - g(f(\mathbf{H}_i, \theta_e), \theta_d)\|^2.$$

- CNN-based autoencoder for learned CSI compression and feedback [3]

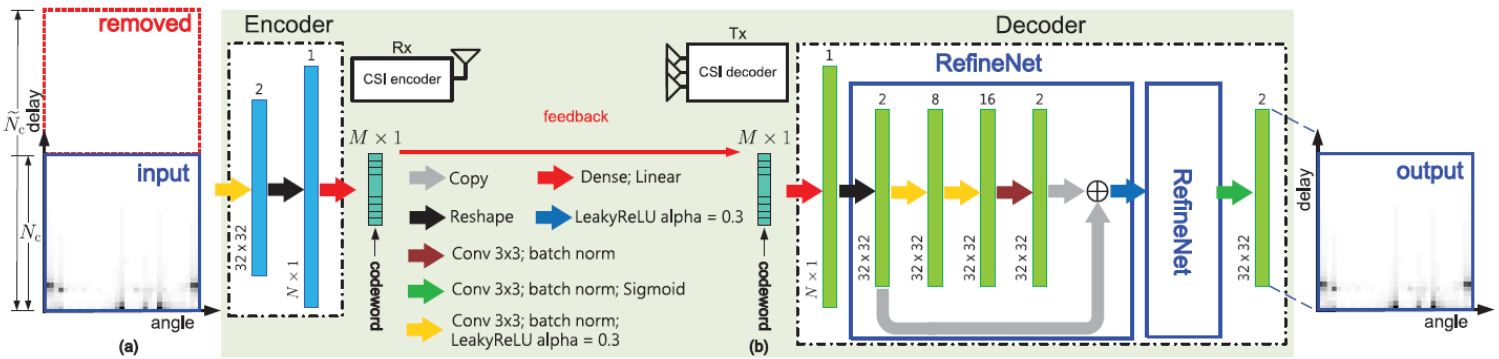

C. Wen, W. Shih, and S. Jin, "Deep Learning for Massive MIMO CSI Feedback," *IEEE Wireless Communications Letters*, vol. 7, pp. 748–751, Oct 2018

Metrics used are:

- **Normalized Mean-squared Error**

$$\text{NMSE} = \frac{1}{N}\sum_{i}^{N}\frac{\|\mathbf{H}_i - \hat{\mathbf{H}}_i\|_F^2}{\|\mathbf{H}_i\|_F^2}$$

- **Cosine Similarity**

$$\rho = \frac{1}{NN_f}\sum_{t=1}^{N}\sum_{n=1}^{N_f}\frac{|\hat{\bar{\mathbf{h}}}_m^H \bar{\mathbf{h}}_m|}{\|\hat{\bar{\mathbf{h}}}_m\|_F \|\bar{\mathbf{h}}_m\|_F},$$

C. Wen, W. Shih, and S. Jin, "Deep Learning for Massive MIMO CSI Feedback," *IEEE Wireless Communications Letters*, vol. 7, pp. 748–751, Oct 2018

CsiNet vs. Compressed Sensing

Metrics used are:

- **Normalized Mean-squared Error**

$$\text{NMSE} = \frac{1}{N}\sum_{i}^{N}\frac{\|\mathbf{H}_i - \hat{\mathbf{H}}_i\|_F^2}{\|\mathbf{H}_i\|_F^2}$$

- **Cosine Similarity**

$$\rho = \frac{1}{NN_f}\sum_{t=1}^{N}\sum_{n=1}^{N_f}\frac{|\hat{\bar{\mathbf{h}}}_m^H \bar{\mathbf{h}}_m|}{\|\hat{\bar{\mathbf{h}}}_m\|_F \|\bar{\mathbf{h}}_m\|_F},$$

CNN-based approaches outperform CS-based approaches at comparable compression ratios.

γ	Methods	Indoor		Outdoor	
		NMSE	ρ	NMSE	ρ
1/4	LASSO	-7.59	0.91	-5.08	0.82
	BM3D-AMP	-4.33	0.80	-1.33	0.52
	TVAL3	-14.87	0.97	-6.90	0.88
	CS-CsiNet	-11.82	0.96	-6.69	0.87
	CsiNet	**-17.36**	**0.99**	**-8.75**	**0.91**
1/16	LASSO	-2.72	0.70	-1.01	0.46
	BM3D-AMP	0.26	0.16	0.55	0.11
	TVAL3	-2.61	0.66	-0.43	0.45
	CS-CsiNet	-6.09	0.87	-2.51	0.66
	CsiNet	**-8.65**	**0.93**	**-4.51**	**0.79**
1/32	LASSO	-1.03	0.48	-0.24	0.27
	BM3D-AMP	24.72	0.04	22.66	0.04
	TVAL3	-0.27	0.33	0.46	0.28
	CS-CsiNet	-4.67	0.83	-0.52	0.37
	CsiNet	**-6.24**	**0.89**	**-2.81**	**0.67**
1/64	LASSO	-0.14	0.22	-0.06	0.12
	BM3D-AMP	0.22	0.04	25.45	0.03
	TVAL3	0.63	0.11	0.76	0.19
	CS-CsiNet	-2.46	0.68	-0.22	0.28
	CsiNet	**-5.84**	**0.87**	**-1.93**	**0.59**

C. Wen, W. Shih, and S. Jin, "Deep Learning for Massive MIMO CSI Feedback," *IEEE Wireless Communications Letters*, vol. 7, pp. 748–751, Oct 2018

CNNs for CSI Estimation

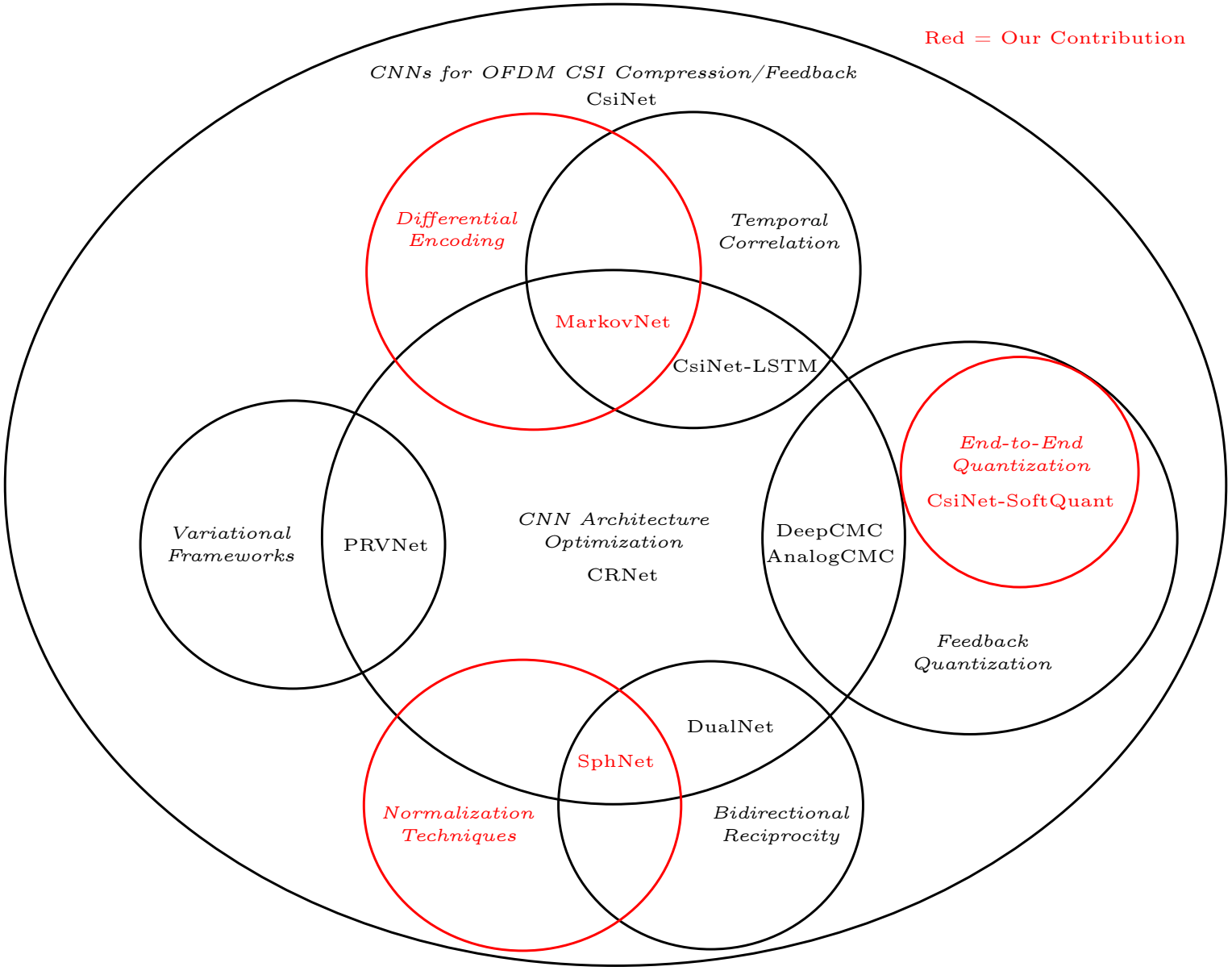

Prior Work #1: SphNet

Power-based normalization for improved CSI reconstruction accuracy.

CsiNet: Minmax Normalization

- **Minmax scaling** for typical works
- Take extrema $(H_{\min}, H_{\max})$ of real and imaginary channels.
- $H_{n,(i,j)} = (i,j)$-th element of n-th sample

$$H_{\text{minmax},n,(i,j)} = \frac{H_{n,(i,j)} - H_{\min}}{H_{\max} - H_{\min}} \in [0,1]$$

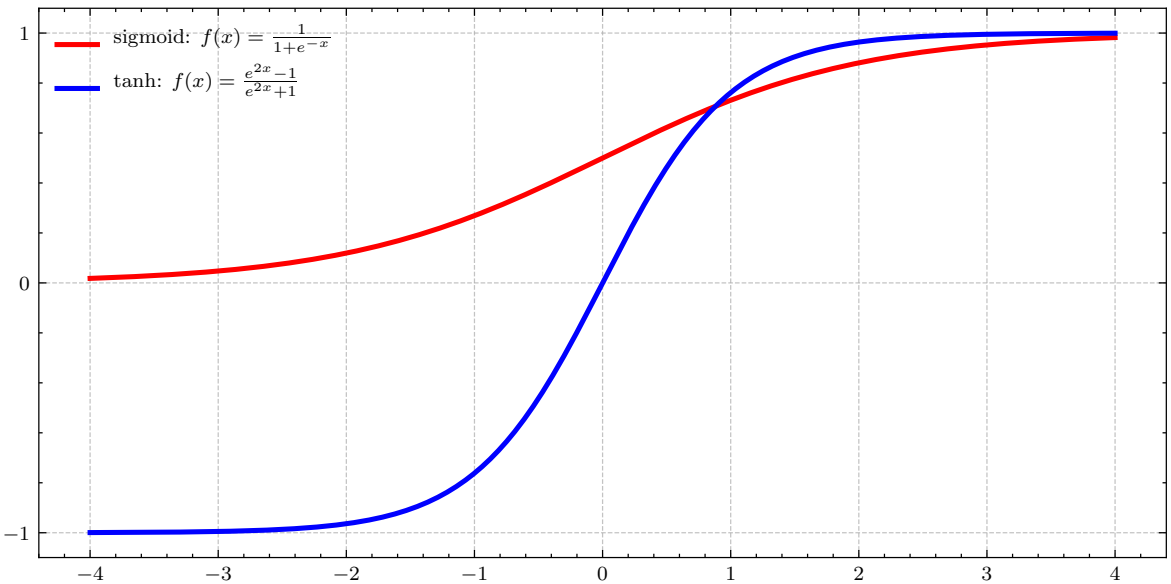

CsiNet: Minmax Normalization

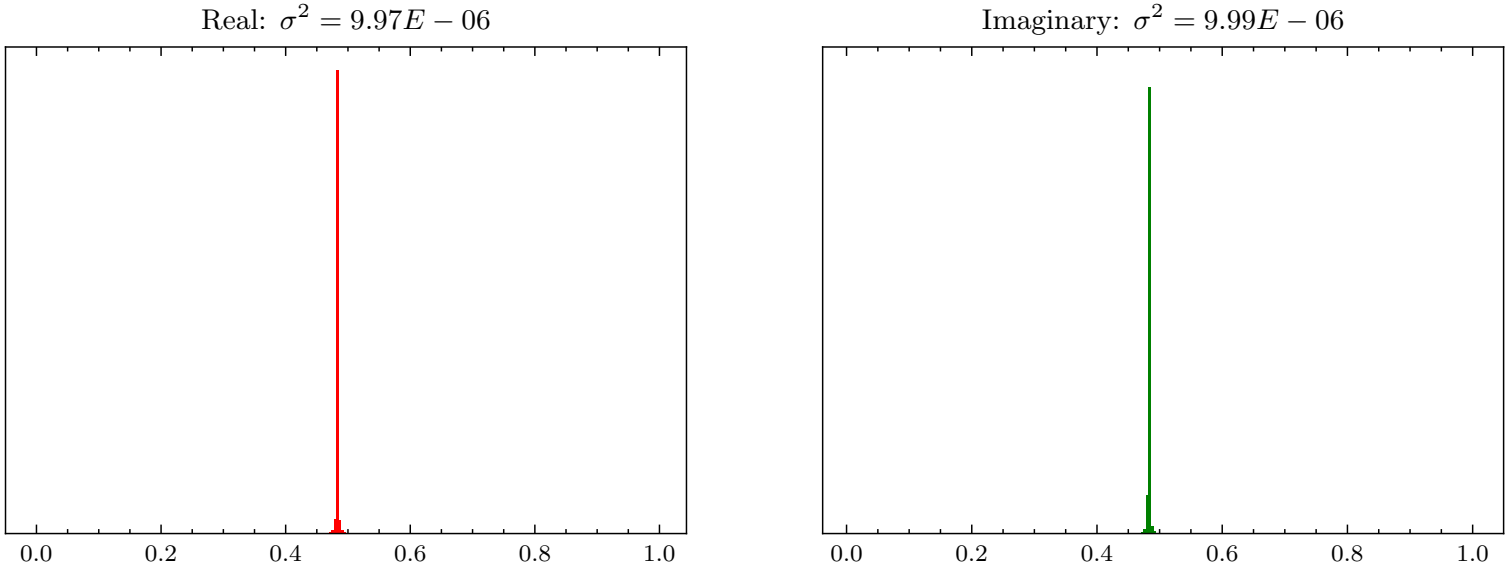

Figure: Distribution and variance of minmax-normalized COST2100 real/imaginary channels ($N = 99000$) images.

ImageNet: Minmax Normalization

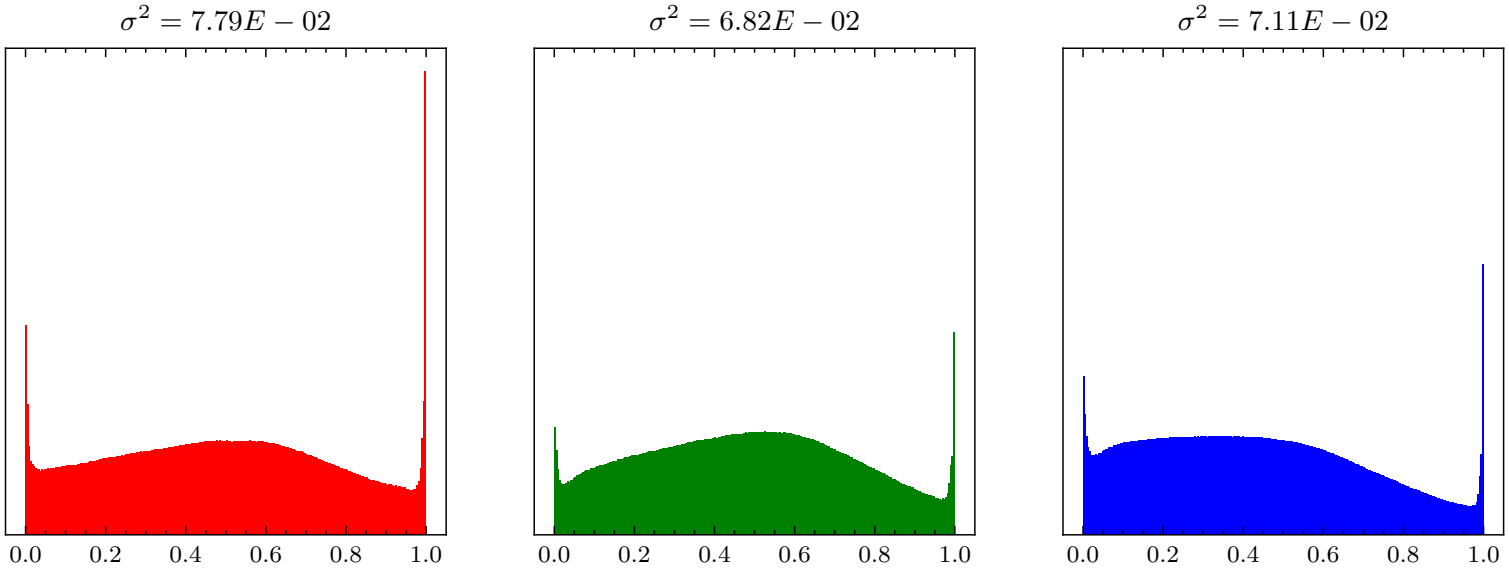

Figure: Distribution and variance of minmax-normalized ImageNet color channels ($N = 50000$) images.

Difference of **four orders of magnitude**.

Dataset	**Channels**	**Normalization**	**Avg. Variance**
ImageNet	RGB	Minmax	$\underline{7.24E^{-2}}$
COST2100	Real, Imag	Minmax	$\underline{9.98E^{-6}}$

Table: Minmax normalization applied to COST2100 and ImageNet dataset.

Spherical normalization – scale each channel sample by its power. For Frobenius norm $\|\cdot\|$,

$$\check{\mathbf{H}}^n = \frac{\mathbf{H}^n}{\|\mathbf{H}^n\|}. \tag{1}$$

Then apply minmax scaling to the entire dataset.

Spherical Normalization

Resulting dataset under spherical normalization exhibits a larger variance than minmax scaling.

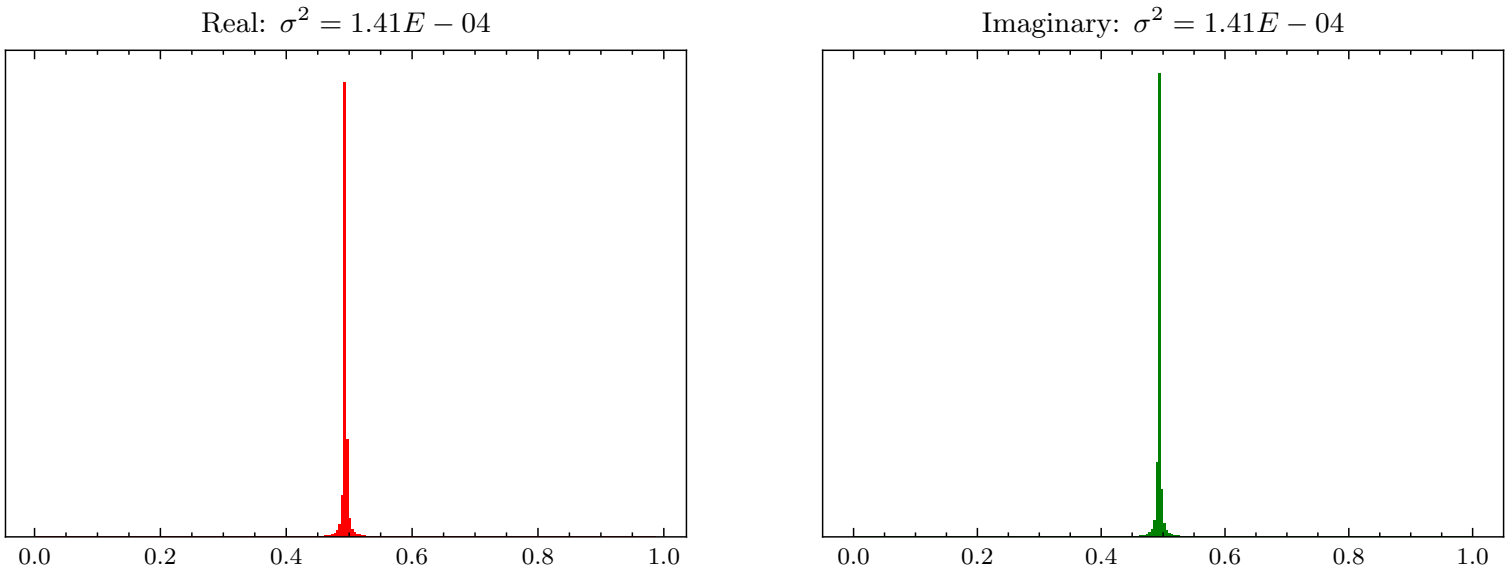

Figure: Distribution/variance of COST2100 real/imaginary channels under spherical normalization ($N = 99000$) images.

Comparison: Spherical vs. Minmax Normalization

Difference is now **two orders of magnitude**.

Dataset	**Channels**	**Normalization**	**Avg. Variance**
ImageNet	RGB	Minmax	$\underline{7.24E^{-2}}$
COST2100	Real, Imag	Spherical	$\underline{1.41E^{-4}}$
COST2100	Real, Imag	Minmax	$9.98E^{-6}$

Table: Minmax vs. spherical normalization applied to COST2100 datasets compared with ImageNet.

MSE/NMSE equivalence

Under spherical normalization, MSE loss becomes equivalent to NMSE. Recall the definitions,

$$\text{MSE} = \frac{1}{N}\sum_{k=1}^{N} \|\mathbf{H}_k - \hat{\mathbf{H}}_k\|^2, \quad \text{NMSE} = \frac{1}{N}\sum_{k=1}^{N} \frac{\|\mathbf{H}_k - \hat{\mathbf{H}}_k\|^2}{\|\mathbf{H}_k\|}$$

Under spherical normalization, MSE loss becomes equivalent to NMSE. Recall the definitions,

$$\text{MSE} = \frac{1}{N}\sum_{k=1}^{N} \|\mathbf{H}_k - \hat{\mathbf{H}}_k\|^2, \quad \text{NMSE} = \frac{1}{N}\sum_{k=1}^{N} \frac{\|\mathbf{H}_k - \hat{\mathbf{H}}_k\|^2}{\|\mathbf{H}_k\|}$$

The MSE of the spherically normalized estimator is equivalent to the NMSE of the regular estimator, i.e.

$$\begin{aligned}
\text{MSE}_{\text{Sph}} &= \frac{1}{N}\sum_{k=1}^{N} \|\check{\mathbf{H}}_k - \hat{\check{\mathbf{H}}}_k\|^2 \\
&= \frac{1}{N}\sum_{k=1}^{N} \left\| \frac{\mathbf{H}_k}{\|\mathbf{H}_k\|} - \frac{\hat{\mathbf{H}}_k}{\|\mathbf{H}_k\|} \right\|^2 \\
&= \frac{1}{N}\sum_{k=1}^{N} \frac{\|\mathbf{H}_k - \hat{\mathbf{H}}_k\|^2}{\|\mathbf{H}_k\|} \square.
\end{aligned}$$

SphNet Architecture

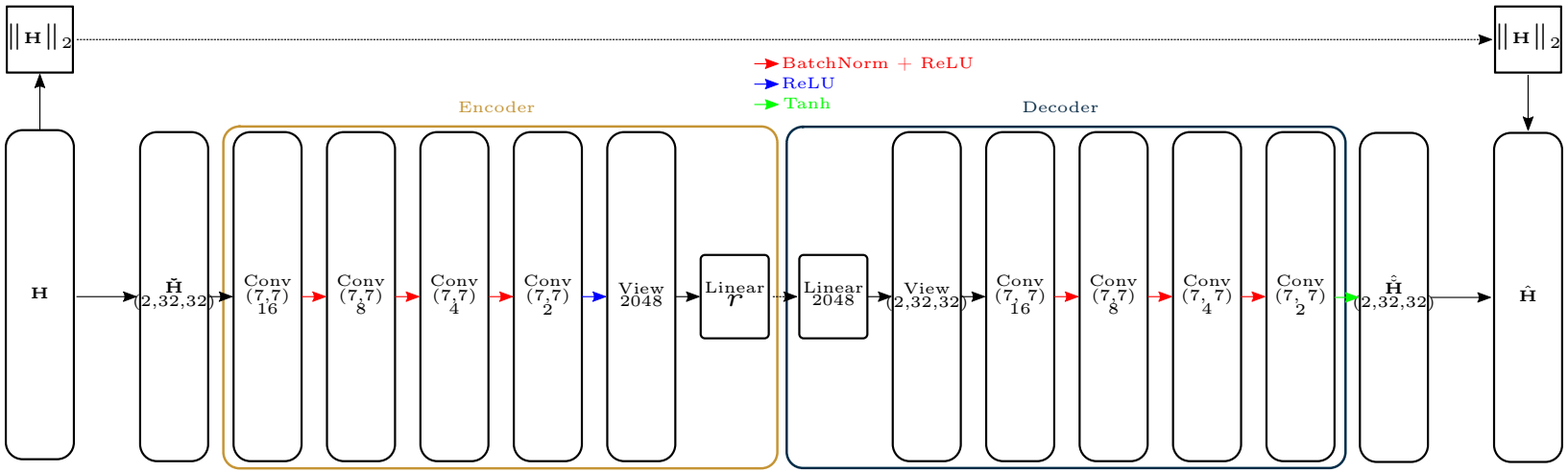

Figure: SphNet – CsiNetPro architecture with Spherical Normalization.

Z. Liu, **M. del Rosario**, X. Liang, L. Zhang, and Z. Ding, "Spherical Normalization for Learned Compressive Feedback in Massive MIMO CSI Acquisition," in *2020 IEEE International Conference on Communications Workshops (ICC Workshops)*, pp. 1–6, 2020

DualNet-Sph Architecture

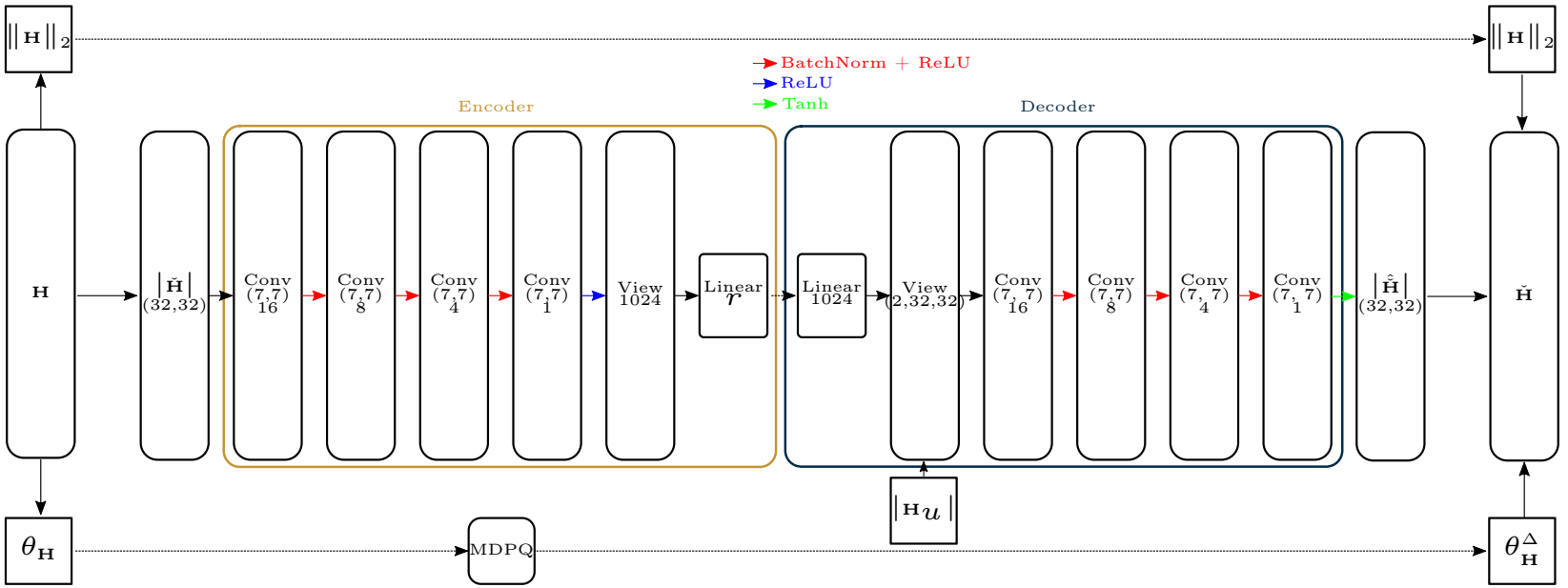

Figure: DualNet-Sph – CsiNetPro architecture with Spherical Normalization and Bidirectional Reciprocity.

Z. Liu, L. Zhang, and Z. Ding, "Exploiting Bi-Directional Channel Reciprocity in Deep Learning for Low Rate Massive MIMO CSI Feedback," *IEEE Wireless Communications Letters*, vol. 8, no. 3, pp. 889–892, 2019

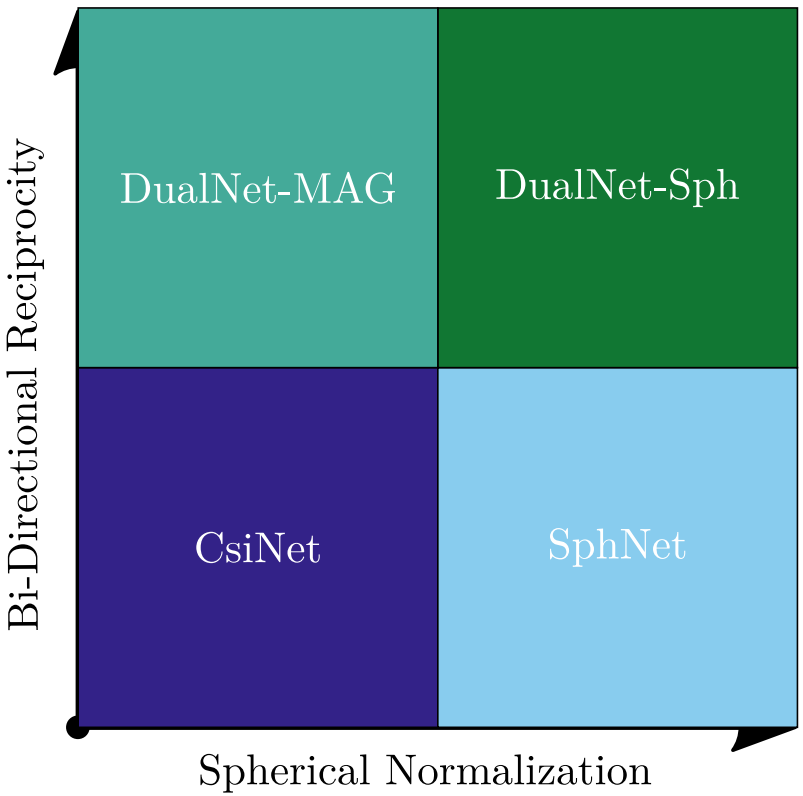

Figure: Illustration of techniques used in different models.

Z. Liu, **M. del Rosario**, X. Liang, L. Zhang, and Z. Ding, "Spherical Normalization for Learned Compressive Feedback in Massive MIMO CSI Acquisition," in *2020 IEEE International Conference on Communications Workshops (ICC Workshops)*, pp. 1–6, 2020

Table: Parameters for COST2100 model in this work.

Environment	**Indoor**	**Outdoor**
Num. gNB Antennas (N_T)	32	
Num. Subcarriers (N_f)	1024	
Carrier Frequency	5.3 GHz	300 MHz
UE Mobility	0.001 m/s	1 m/s
UE Starting Position	20×20 m	400×400 m
Num. Channel Samples (N)	10^5	
Training/Validation Split	70%/30%	
Feedback interval	40 ms	

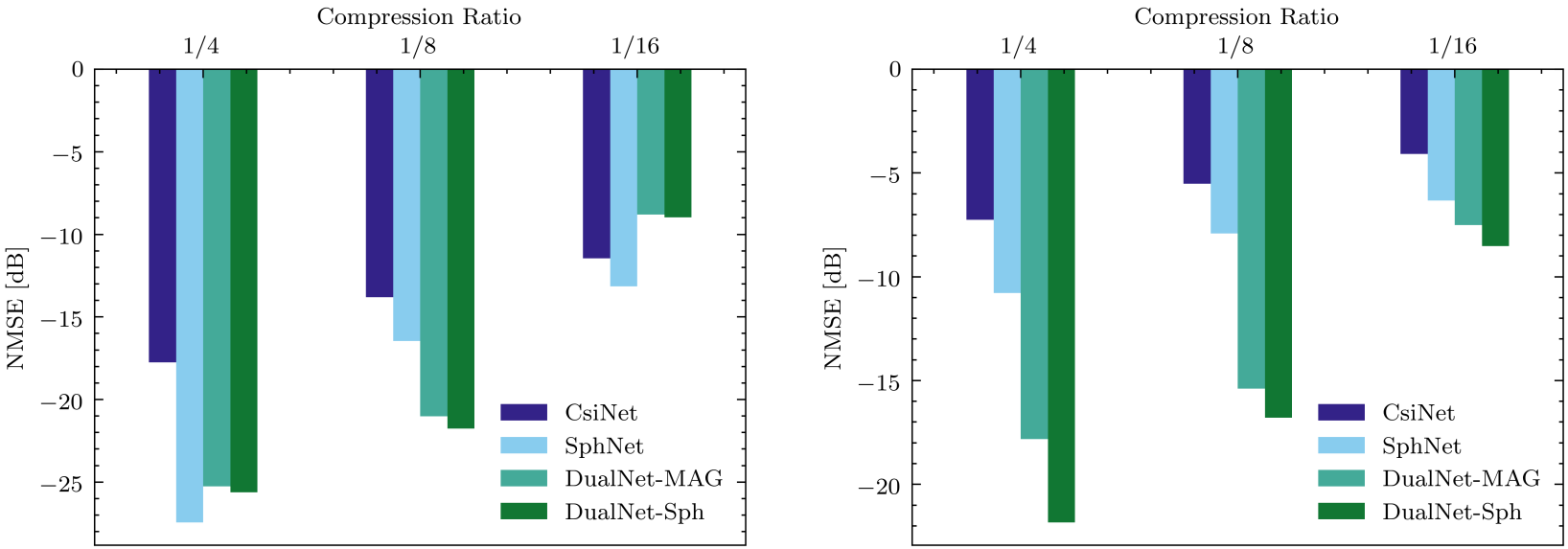

(a) Indoor (b) Outdoor

Figure: NMSE (lower is better) comparison of bidirectional reciprocity and spherical normalization against CsiNet for increasing compression ratio [4]

Z. Liu, **M. del Rosario**, X. Liang, L. Zhang, and Z. Ding, "Spherical Normalization for Learned Compressive Feedback in Massive MIMO CSI Acquisition," in *2020 IEEE International Conference on Communications Workshops (ICC Workshops)*, pp. 1–6, 2020

Prior Work #2: MarkovNet

A deep differential autoencoder for efficient temporal learning.

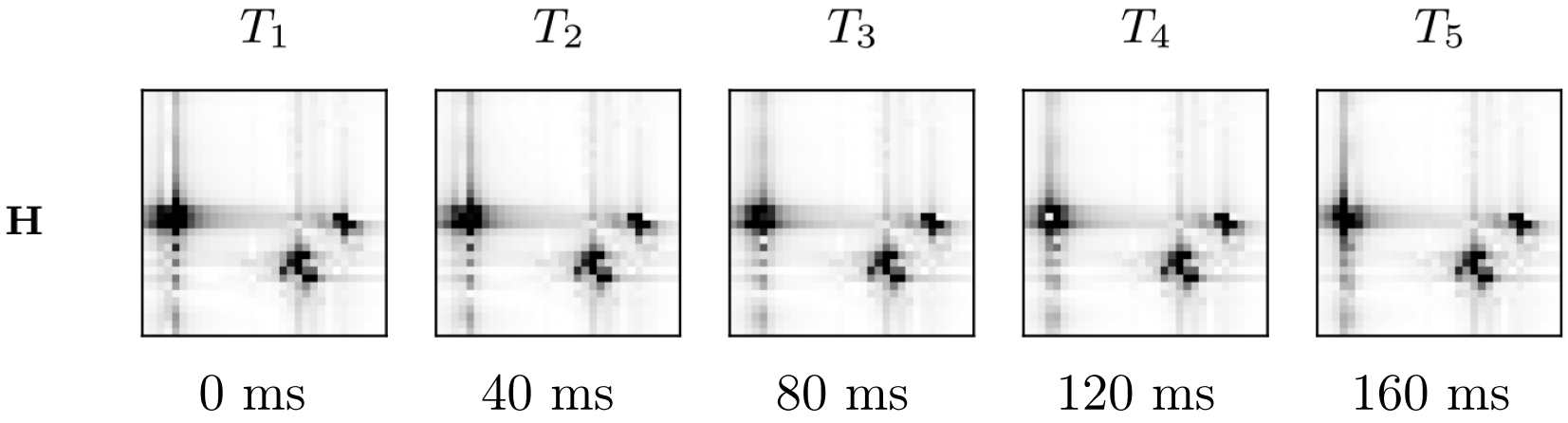

Figure: Ground truth CSI (**H**) for five timeslots (T_1 through T_5) on one outdoor sample from the validation set.

Recurrent neural networks (RNNs) contain trainable long short-term memory (LSTM) cells which learn temporal relationships.

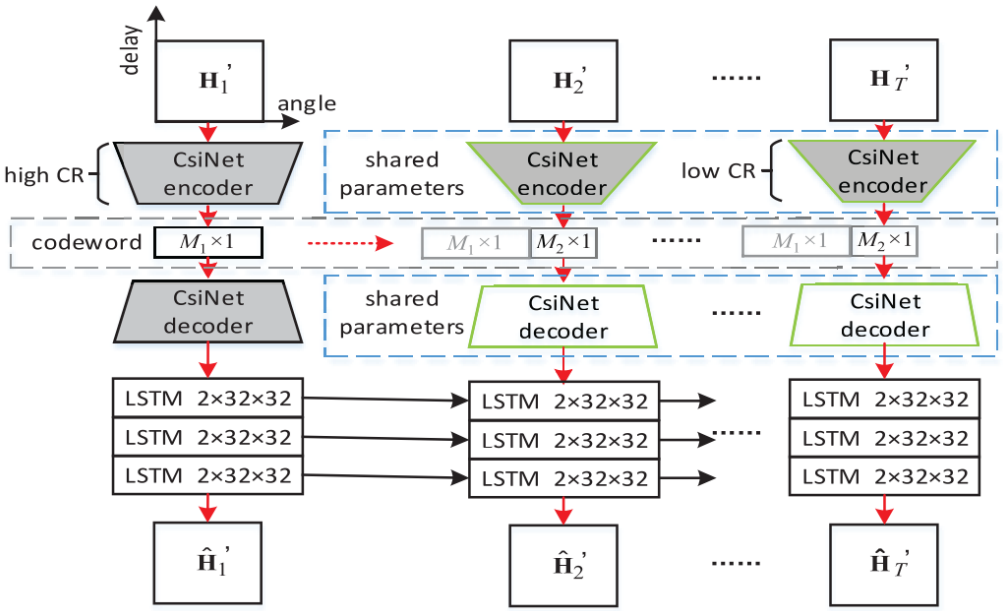

Figure: CsiNet-LSTM network architecture [6].

T. Wang, C. Wen, S. Jin, and G. Y. Li, "Deep Learning-Based CSI Feedback Approach for Time-Varying Massive MIMO Channels," *IEEE Wireless Comm. Letters*, vol. 8, pp. 416–419, April 2019

CsiNet-LSTM Performance

LSTMs improve NMSE at smaller compression ratios.

		CR	LASSO	BM3D-AMP	TVAL3	CsiNet	CsiNet-LSTM
Indoor	NMSE	1/16	-2.96	0.25	-3.20	-10.59	**-23.06**
		1/32	-1.18	20.85	-0.46	-7.35	**-22.33**
		1/64	-0.18	26.66	0.60	-6.09	**-21.24**
	ρ	1/16	0.72	0.29	0.73	0.95	**0.99**
		1/32	0.53	0.17	0.45	0.90	**0.99**
		1/64	0.30	0.16	0.24	0.87	**0.99**
	runtime	1/16	0.2471	0.3454	0.3148	**0.0001**	0.0003
		1/32	0.2137	0.5556	0.3148	**0.0001**	0.0003
		1/64	0.2479	0.6047	0.2860	**0.0001**	0.0003
	NMSE↓	1/16-1/64	94%	105	1.19	42%	**8%**
Outdoor	NMSE	1/16	-1.09	0.40	-0.53	-3.60	**-9.86**
		1/32	-0.27	18.99	0.42	-2.14	**-9.18**
		1/64	-0.06	24.42	0.74	-1.65	**-8.83**
	ρ	1/16	0.49	0.23	0.46	0.75	**0.95**
		1/32	0.32	0.16	0.28	0.63	**0.94**
		1/64	0.19	0.16	0.19	0.58	**0.93**
	runtime	1/16	0.2122	0.4210	0.3145	**0.0001**	0.0003
		1/32	0.2409	0.6031	0.2985	**0.0001**	0.0003
		1/64	0.0166	0.5980	0.2850	**0.0001**	0.0003
	NMSE↓	1/16-1/64	94%	60	2.40	54%	**10%**

T. Wang, C. Wen, S. Jin, and G. Y. Li, "Deep Learning-Based CSI Feedback Approach for Time-Varying Massive MIMO Channels," *IEEE Wireless Comm. Letters*, vol. 8, pp. 416–419, April 2019

Problem: Number of parameters/FLOPs for RNNs is large.

Table: Model size/computational complexity per timeslot for CsiNet-LSTM and CsiNet. M: million.

	Parameters		**FLOPs**	
CR	**CsiNet-LSTM**	**CsiNet**	**CsiNet-LSTM**	**CsiNet**
1/4	132.7 M	2.1 M	412.9 M	7.8 M
1/8	123.2 M	1.1 M	410.8 M	5.7 M
1/16	118.5 M	0.5 M	409.8 M	4.7 M
1/32	116.1 M	0.3 M	409.2 M	4.1 M
1/64	115.0 M	0.1 M	409.0 M	3.9 M

Markov Assumption

Instead of learning a temporal dependency across multiple timeslots, we proposed a **one-step differential encoder**.

For short enough feedback intervals between t and $t-1$, we view CSI data as a Markov chain, i.e.

$$\mathbf{H}_t = \gamma \mathbf{H}_{t-1} + \mathbf{V}_t,$$

with $\gamma \in \mathbb{R}^+$ and i.i.d $\mathbf{V}_t$ such that $\mathbf{V}_t \sim \mathcal{CN}(\mathbf{0}, \Sigma_V)$.

Z. Liu †, **M. del Rosario †**, and Z. Ding, "A Markovian Model-Driven Deep Learning Framework for Massive MIMO CSI Feedback," *arXiv e-prints*, Sept. 2020. Submitted to IEEE Transactions on Wireless Communications († equal contribution)

The ordinary least-squares solution, γ, is given as

$$\gamma = \frac{\text{Trace}(\mathbb{E}\left[\mathbf{H}_{t-1}^{H}\mathbf{H}_{t}\right])}{\mathbb{E}\|\mathbf{H}_{t}^{H}\mathbf{H}_{t}\|^{2}}.$$

The ordinary least-squares solution, γ, is given as

$$\gamma = \frac{\text{Trace}(\mathbb{E}\left[\mathbf{H}_{t-1}^H \mathbf{H}_t\right])}{\mathbb{E}\|\mathbf{H}_t^H \mathbf{H}_t\|^2}.$$

We utilize the estimator, $\hat{\gamma}$, based on the second-order statistics of the CSI matrices,

$$\hat{\gamma} = \frac{\sum_{i=1}^{N} \text{Trace}(\left[\mathbf{H}_{t-1}^H(i)\mathbf{H}_t(i)\right])}{\sum_{i=1}^{N} \|\mathbf{H}_t^H(i)\mathbf{H}_t(i)\|^2},$$

for training set of size N.

With the one-step estimator $\hat{\gamma}$, we propose train an encoder for the estimation error as

$$\mathbf{z}_t = f_{e,t}(\mathbf{H}_t - \hat{\gamma}\hat{\mathbf{H}}_{t-1}),$$

and we jointly train a decoder,

$$\hat{\mathbf{H}}_t = f_{d,t}(\mathbf{z}_t) + \hat{\gamma}\hat{\mathbf{H}}_{t-1}$$

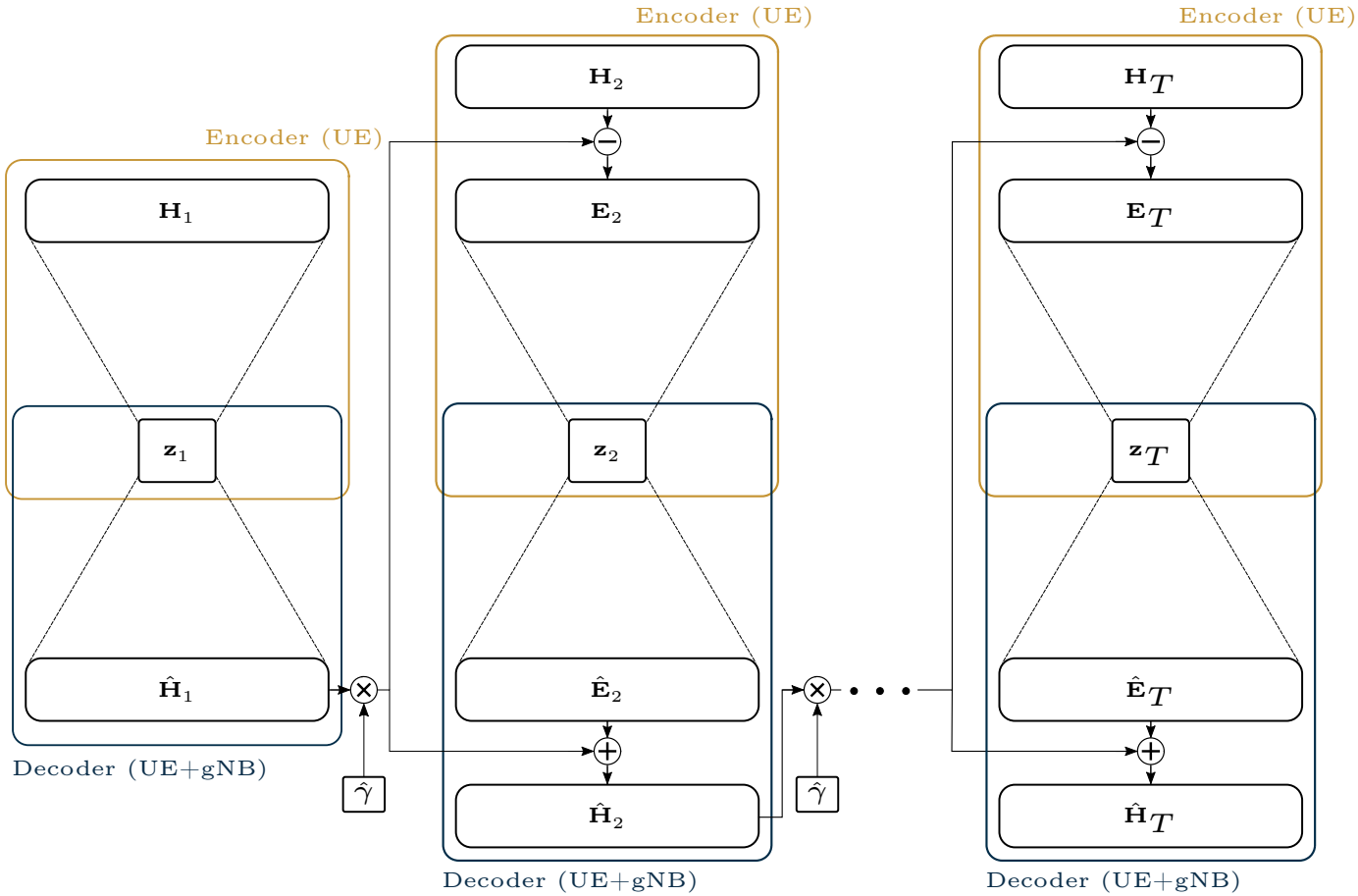

Figure: Abstract architecture for MarkovNet. Networks at $t \geq 2$ are trained to predict the estimation error, $\mathbf{E}_t$.

MarkovNet Results – NMSE Performance

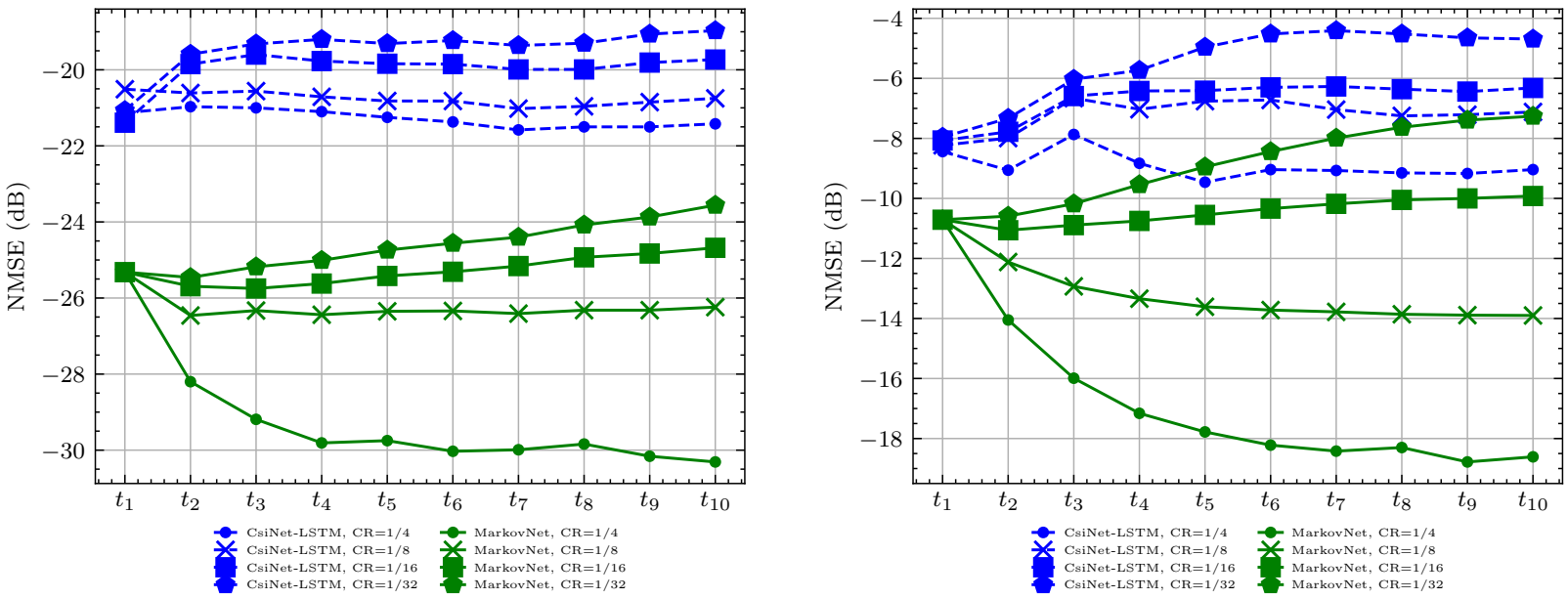

(a) Indoor (b) Outdoor

Figure: NMSE comparison of MarkovNet and CsiNet-LSTM at various compression ratios (CR).

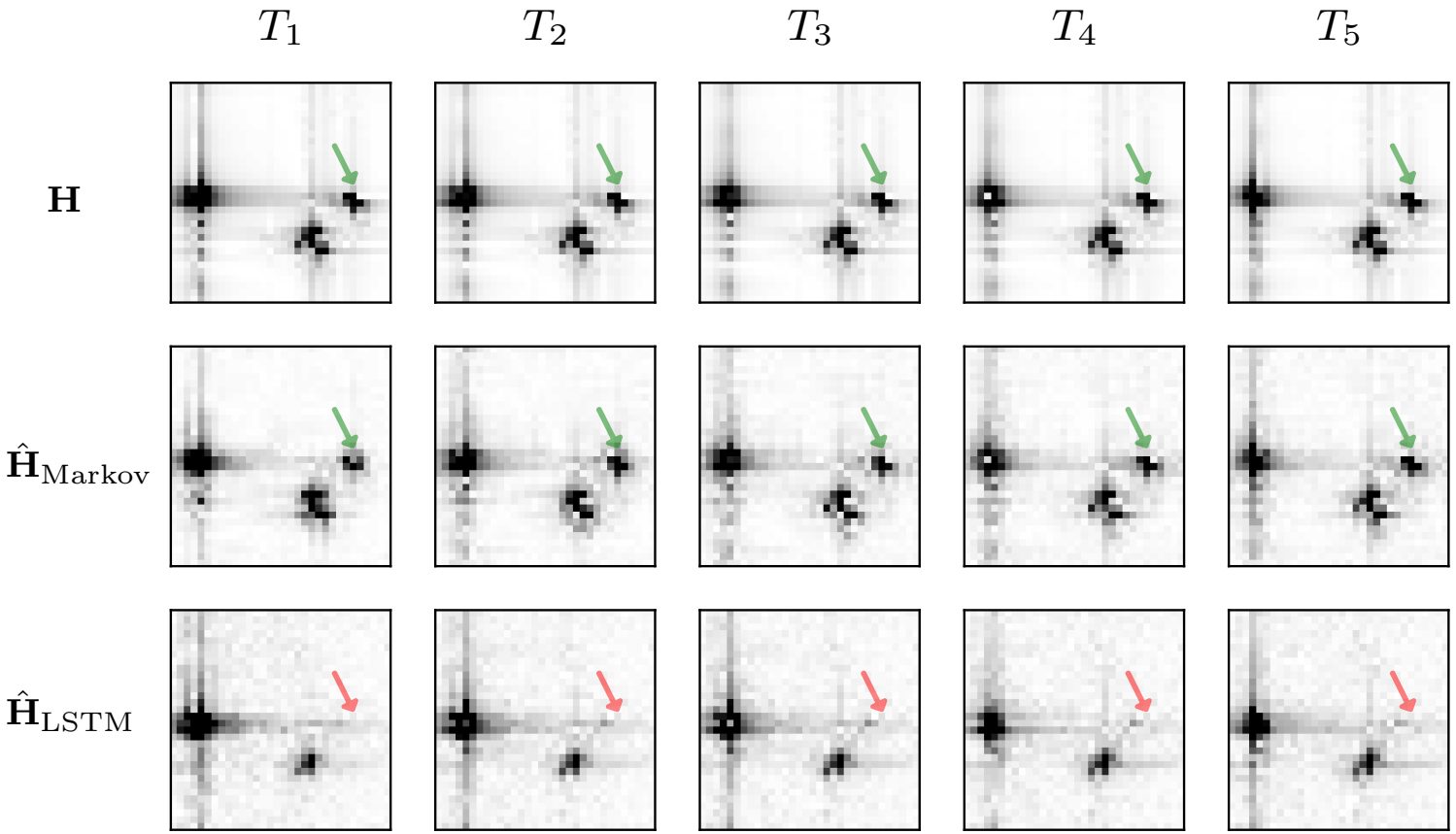

Figure: Ground truth CSI ($\mathbf{H}$), MarkovNet estimates ($\hat{\mathbf{H}}_{\text{Markov}}$), and CsiNet-LSTM estimates ($\hat{\mathbf{H}}_{\text{LSTM}}$) for five timeslots ($T_1$ through T_5) on one outdoor sample from the test set (both networks at CR $= \frac{1}{4}$).

Table: Model size/computational complexity of tested temporal networks (CsiNet-LSTM, MarkovNet) and comparable non-temporal network (CsiNet). M: million.

	Parameters		
	CsiNet-LSTM	**MarkovNet**	**CsiNet**
CR=1/4	132.7 M	2.1 M	2.1 M
CR=1/8	123.2 M	1.1 M	1.1 M
CR=1/16	118.5 M	0.5 M	0.5 M
CR=1/32	116.1 M	0.3 M	0.3 M
CR=1/64	115.0 M	0.1 M	0.1 M
	FLOPs		
	CsiNet-LSTM	**MarkovNet**	**CsiNet**
CR=1/4	412.9 M	44.5 M	7.8 M
CR=1/8	410.8 M	42.4 M	5.7 M
CR=1/16	409.8 M	41.3 M	4.7 M
CR=1/32	409.2 M	40.8 M	4.1 M
CR=1/64	409.0 M	40.5 M	3.9 M

Proposed Work: CsiNet-SoftQuant

An end-to-end trained autoencoder with learned feedback quantization.

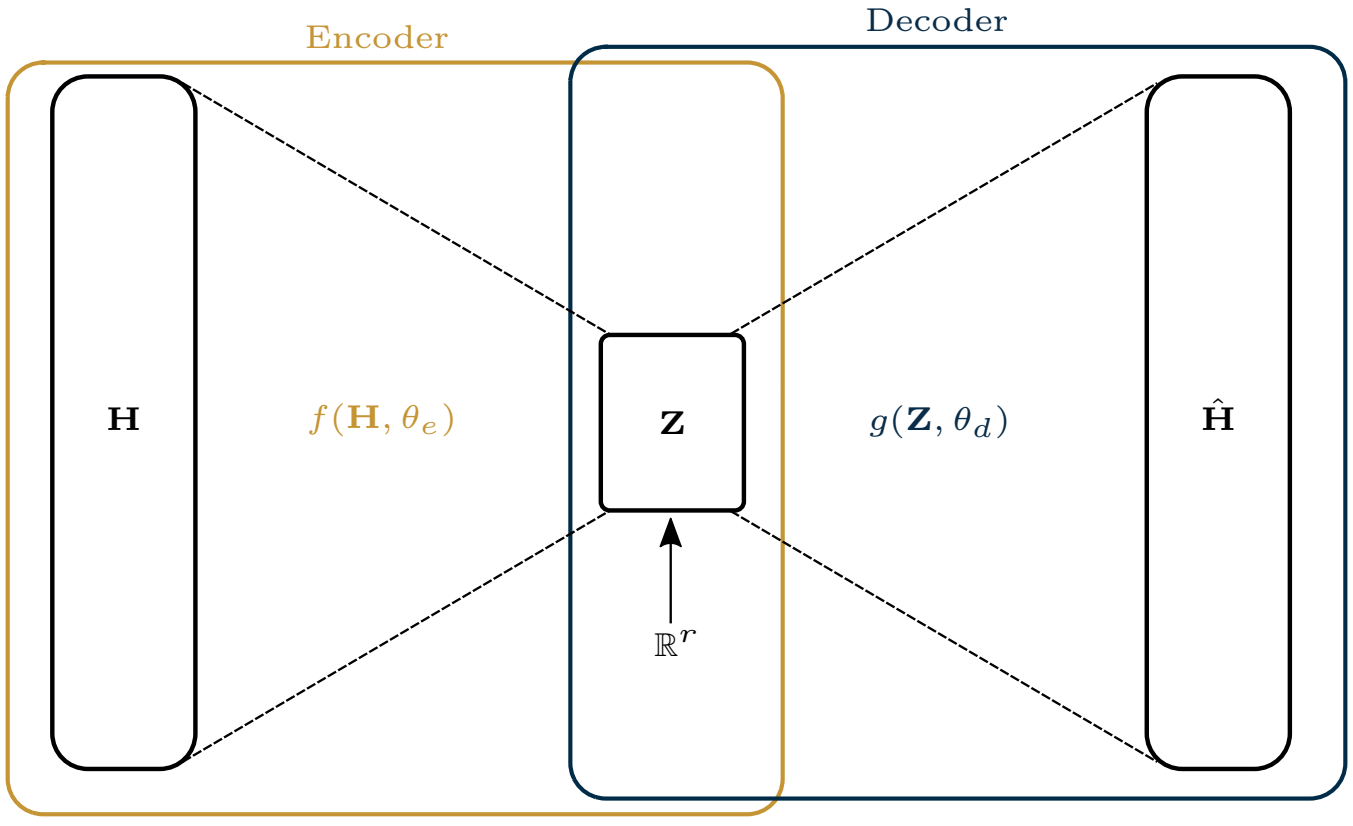

Figure: Autoencoder architecture with r-dimensional real-valued latent feedback elements.

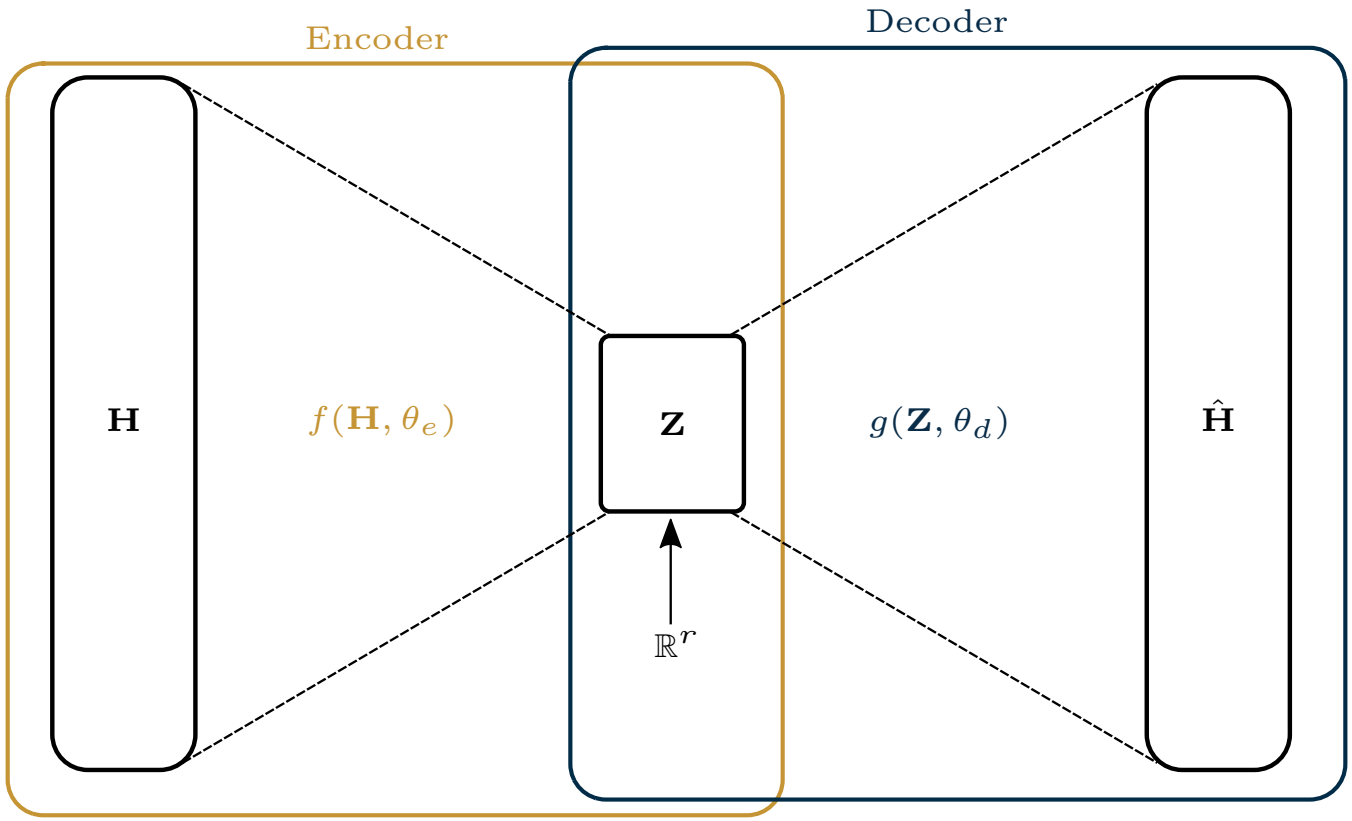

Figure: Autoencoder architecture with r-dimensional real-valued latent feedback elements.

Problem: Feedback elements must be discrete-valued. How to quantize?

Network with uniform quantization and arithmetic encoding of latent vectors.

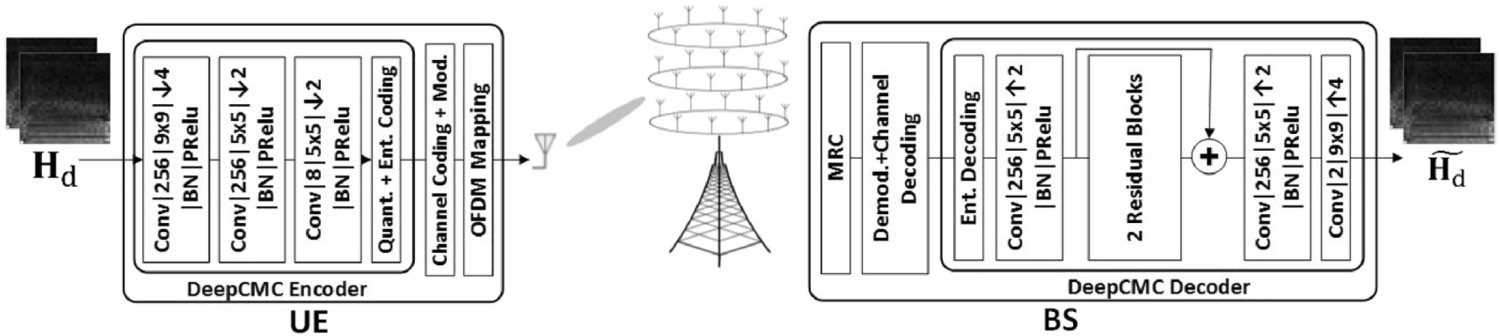

Figure: Architecture for DeepCMC [8]. Network uses entropy encoding of uniform quantized feedback elements to minimize bit rate.

Q. Yang, M. B. Mashhadi, and D. Gündüz, "Deep Convolutional Compression For Massive MIMO CSI Feedback," in *2019 IEEE 29th International Workshop on Machine Learning for Signal Processing (MLSP)*, pp. 1–6, 2019

Network with uniform quantization and arithmetic encoding of latent vectors.

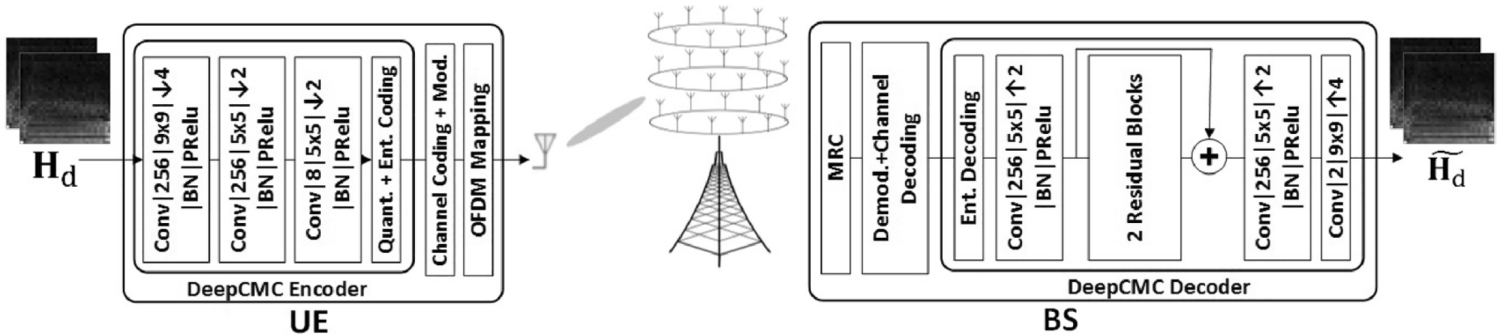

Figure: Architecture for DeepCMC [8]. Network uses entropy encoding of uniform quantized feedback elements to minimize bit rate.

Is fixed quantization scheme optimal?

Q. Yang, M. B. Mashhadi, and D. Gündüz, "Deep Convolutional Compression For Massive MIMO CSI Feedback," in *2019 IEEE 29th International Workshop on Machine Learning for Signal Processing (MLSP)*, pp. 1–6, 2019

Soft Quantization

We propose to use soft-to-hard vector quantization (SHVQ) [9]. Define the m-dimensional codebook of size L as $\mathbf{C} \in \mathbb{R}^{m \times L}$. The soft vector assignments of the j-th latent vector $\tilde{\mathbf{z}}_j$ can be written as,

$$\phi(\tilde{\mathbf{z}}_j) = \left[\frac{\exp(-\sigma \|\tilde{\mathbf{z}}_j - \mathbf{c}_\ell\|^2)}{\sum_{i=1}^{L} \exp(-\sigma \|\tilde{\mathbf{z}}_j - \mathbf{c}_i\|^2)} \right]_{\ell \in [L]} \in \mathbb{R}^L, \tag{2}$$

which is referred to as the 'softmax' function. σ is a *temperature* or *annealing* parameter which controls the degree of quantization,

$$\lim_{\sigma \to \infty} \phi(\tilde{\mathbf{z}}_j) = \text{onehot}(\tilde{\mathbf{z}}_j) = \begin{cases} 1 & \ell = \underset{\ell}{\text{argmax}}\ \phi(\tilde{\mathbf{z}}_j)[\ell] \\ 0 & \text{otherwise} \end{cases} \tag{3}$$

E. Agustsson, F. Mentzer, M. Tschannen, L. Cavigelli, R. Timofte, L. Benini, and L. Van Gool, "Soft-to-hard Vector Quantization for End-to-end Learning Compressible Representations," *Advances in Neural Information Processing Systems*, vol. 2017-Decem, no. NIPS, pp. 1142–1152, 2017

The soft assignments ϕ admit probability masses over the codewords,

$$q_j = \phi(\tilde{\mathbf{z}}_j).$$

Based on finite samples, we define the histogram probability estimates p_j

$$p_j = \frac{|\{e_l(\mathbf{z}_i)|l \in [m], i \in [N], e_l(\mathbf{z}_i) = j\}|}{mN}.$$

Our target for the rate loss is the crossentropy between p_j and q_j term,

$$H(\phi) := H(p, q) = -\sum_{j=1}^{L} p_j \log q_j = H(p) + D_{\mathrm{KL}}(p\|q).$$

E. Agustsson, F. Mentzer, M. Tschannen, L. Cavigelli, R. Timofte, L. Benini, and L. Van Gool, "Soft-to-hard Vector Quantization for End-to-end Learning Compressible Representations," *Advances in Neural Information Processing Systems*, vol. 2017-Decem, no. NIPS, pp. 1142–1152, 2017

Rate-Distortion Loss

Loss function for soft quantization = regularized rate-distortion

$$\underset{\theta_e,\theta_d,\mathbf{C}}{\operatorname{argmin}} \overbrace{L_d(\mathbf{H},\hat{\mathbf{H}})}^{\text{distortion}} + \lambda \overbrace{L_{\ell 2}(\theta_e,\theta_d,\mathbf{C})}^{\ell_2 \text{ penalty}} + \beta \overbrace{L_r(\theta_e,\mathbf{C})}^{\text{rate}} \tag{4}$$

Where the different loss terms are

Term	**Definition**
$L_d(\mathbf{H},\hat{\mathbf{H}})$	$\frac{1}{N}\sum_{i=1}^{N}\|\mathbf{H}_i - g(Q(f(\mathbf{H}_i,\theta_e),\mathbf{C}),\theta_d)\|^2$
$L_{\ell 2}(\theta_e,\theta_d,\mathbf{C})$	$\|\theta_e\|^2 + \|\theta_d\|^2 + \|\mathbf{C}\|^2$
$L_r(\theta_e,\mathbf{C})$	$mH(\phi)$

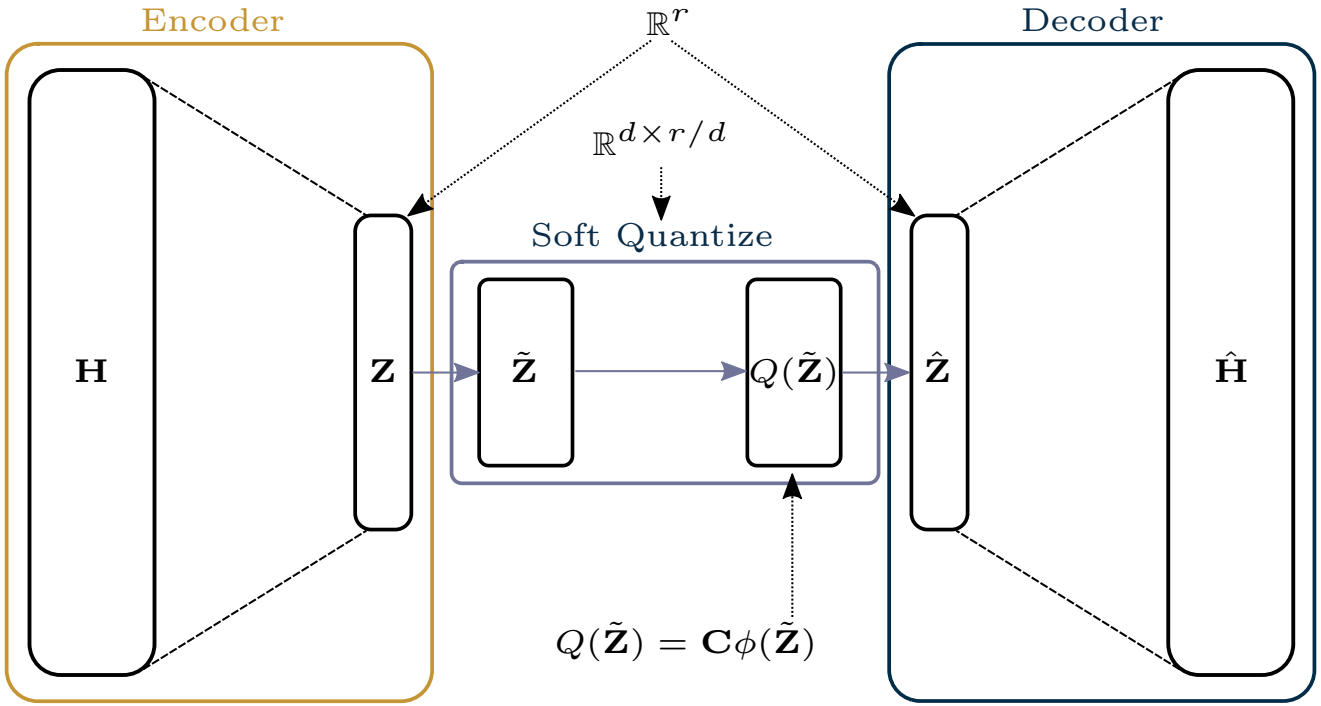

Figure: Abstract architecture for CsiNet-SoftQuant [8]. SoftQuantize layer ($Q(\tilde{\mathbf{Z}})$) is a continuous, softmax-based relaxation of a d-dimensional quantization of the latent layer $\mathbf{Z}$.

Results: Rate-Distortion (Outdoor)

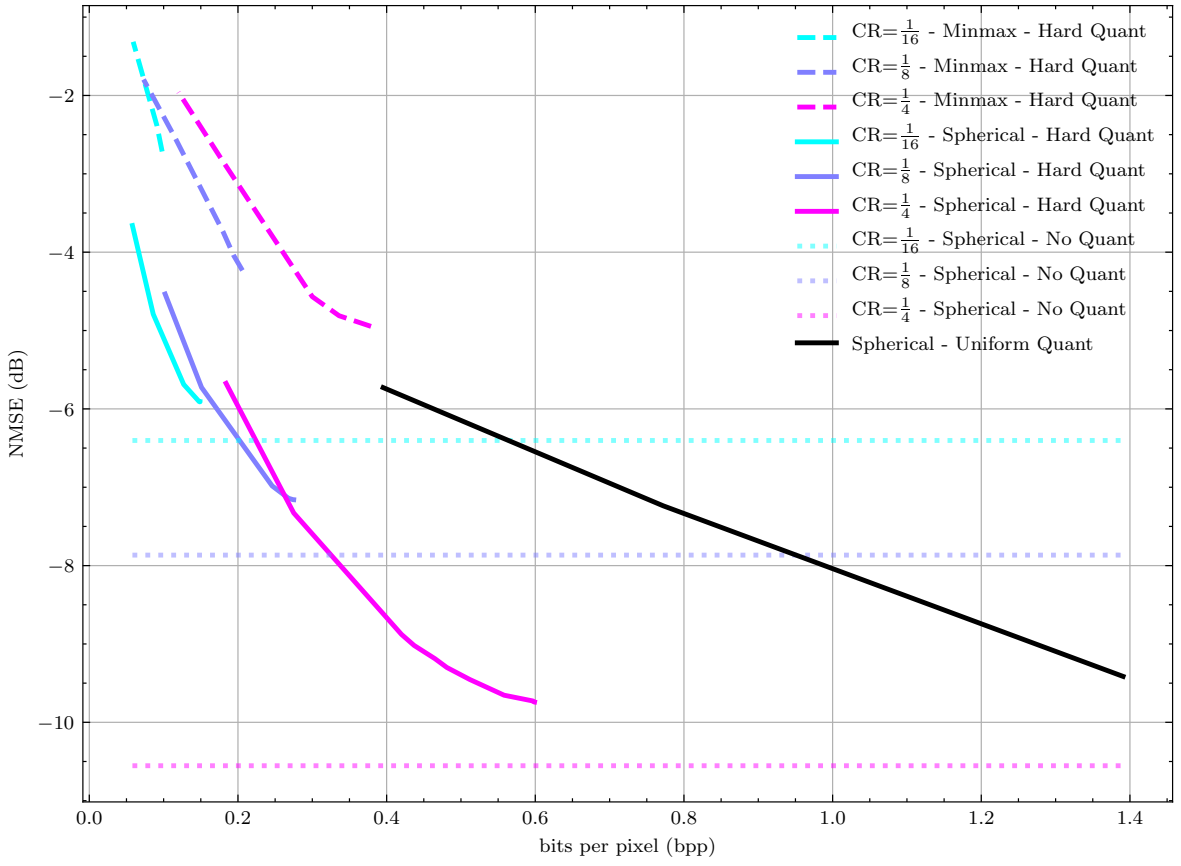

Figure: Rate distortion of CsiNet-SoftQuant under both minmax (dotted line) and spherical (solid line) normalization using: $L = 1024$ centers, $d = 4$. Hard quantization performance shown for each CR.

Given angular-delay domain CSI data, $\mathbf{H}$, assume i.i.d. $\mathbf{H}_{(i,j)}$ for i-th (j-th) row (col).

Given angular-delay domain CSI data, $\mathbf{H}$, assume i.i.d. $\mathbf{H}_{(i,j)}$ for i-th (j-th) row (col).

Denote the quantized CSI matrix, $\mathbf{H}^{\Delta}$, quantized with b bits. The entropy of the (i,j)-th element is

$$H(\mathbf{H}^{\Delta}_{(i,j)}) = -\sum_{k}^{2^b} p(\mathbf{H}^{\Delta}_{(i,j)} = k) \log p(\mathbf{H}^{\Delta}_{(i,j)} = k),$$

where $p(\mathbf{H}^{\Delta}_{(i,j)} = k)$ can be obtained as a histogram estimate over the entire dataset.

Given angular-delay domain CSI data, $\mathbf{H}$, assume i.i.d. $\mathbf{H}_{(i,j)}$ for i-th (j-th) row (col).

Denote the quantized CSI matrix, $\mathbf{H}^{\Delta}$, quantized with b bits. The entropy of the (i,j)-th element is

$$H(\mathbf{H}^{\Delta}_{(i,j)}) = -\sum_{k}^{2^b} p(\mathbf{H}^{\Delta}_{(i,j)} = k) \log p(\mathbf{H}^{\Delta}_{(i,j)} = k),$$

where $p(\mathbf{H}^{\Delta}_{(i,j)} = k)$ can be obtained as a histogram estimate over the entire dataset.

A conservative upper bound on the entropy of the full CSI matrix is

$$H(\mathbf{H}^{\Delta}) = \frac{1}{R_d n_T} \sum_{i}^{R_d} \sum_{j}^{n_T} H(\mathbf{H}^{\Delta}_{(i,j)}).$$

Entropy Estimation: Results

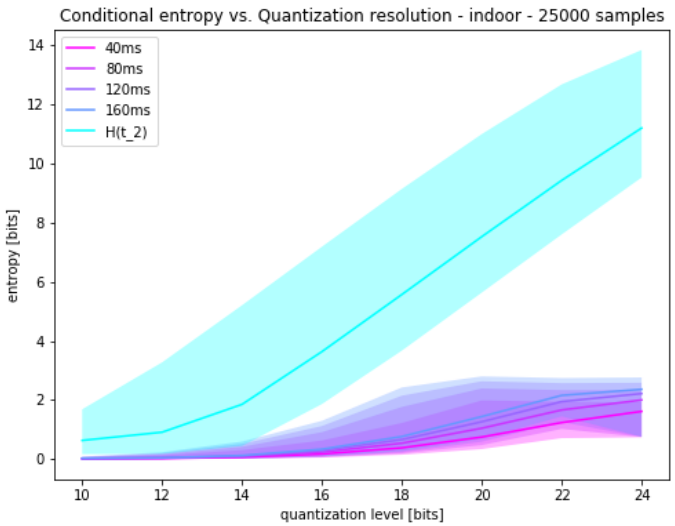

(a) Indoor

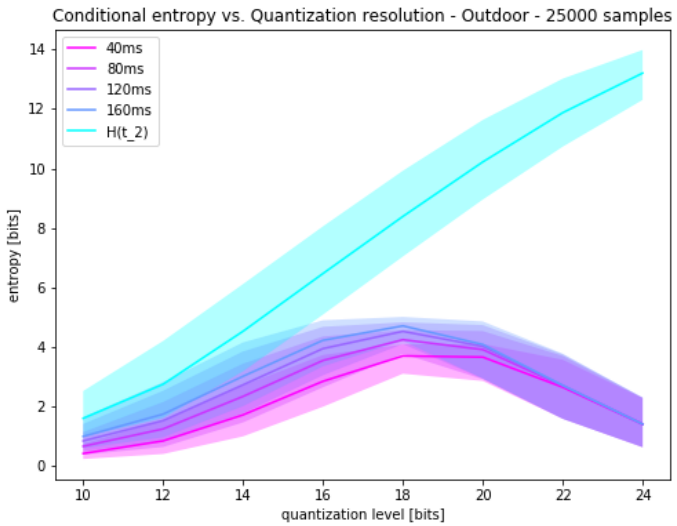

(b) Outdoor

Figure: Mean entropy/conditional entropy estimates $H(\mathbf{H}^{\Delta})$ with 95% c.i. for quantized i.i.d COST2100 elements vs. quantization level (bits).

Again, assume i.i.d. $\mathbf{H}_{(i,j)}$ for i-th (j-th) row (col).

L. Kozachenko and N. N. Leonenko, "Sample Estimate of the Entropy of a Random Vector," *Problemy Peredachi Informatsii*, vol. 23, no. 2, pp. 9–16, 1987

Again, assume i.i.d. $\mathbf{H}_{(i,j)}$ for i-th (j-th) row (col).

The differential entropy of the (i,j)-th element is

$$\hat{h}(\mathbf{H}_{(i,j)}) = -\int p(\mathbf{H}(i,j) = k) \log p(\mathbf{H}_{(i,j)} = k) dk,$$

L. Kozachenko and N. N. Leonenko, "Sample Estimate of the Entropy of a Random Vector," *Problemy Peredachi Informatsii*, vol. 23, no. 2, pp. 9–16, 1987

Again, assume i.i.d. $\mathbf{H}_{(i,j)}$ for i-th (j-th) row (col).

The differential entropy of the (i,j)-th element is

$$\hat{h}(\mathbf{H}_{(i,j)}) = -\int p(\mathbf{H}(i,j)=k)\log p(\mathbf{H}_{(i,j)}=k)dk,$$

$p(\mathbf{H}_{(i,j)})$ is difficult to obtain. Instead resort to Kozachenko–Leonenko (KL) estimator [10] for each element in $\mathbf{H}$ and average over the elements,

$$\hat{h}(\mathbf{H}) = \frac{1}{R_d n_T}\sum_{i}^{R_d}\sum_{j}^{n_T}\hat{h}(\mathbf{H}_{(i,j)}),$$

for KL estimator $\hat{h}$.

L. Kozachenko and N. N. Leonenko, "Sample Estimate of the Entropy of a Random Vector," *Problemy Peredachi Informatsii*, vol. 23, no. 2, pp. 9–16, 1987

Quantized vs. Differential Entropy

Based on Theorem 8.3.1 from Cover [11], – for sufficiently small quantization interval $\Delta = \frac{1}{2^n}$, the entropy of a quantized random variable is related to its differential entropy as,

$$H(\mathbf{H}^{\Delta}) = h(\mathbf{H}) + n,$$

for n-bit quantization. Thus, the differential entropy estimator admits an estimate for the entropy of the quantized CSI, $\hat{\mathbf{H}}^{\Delta}$.

Differential Entropy Estimation: Results

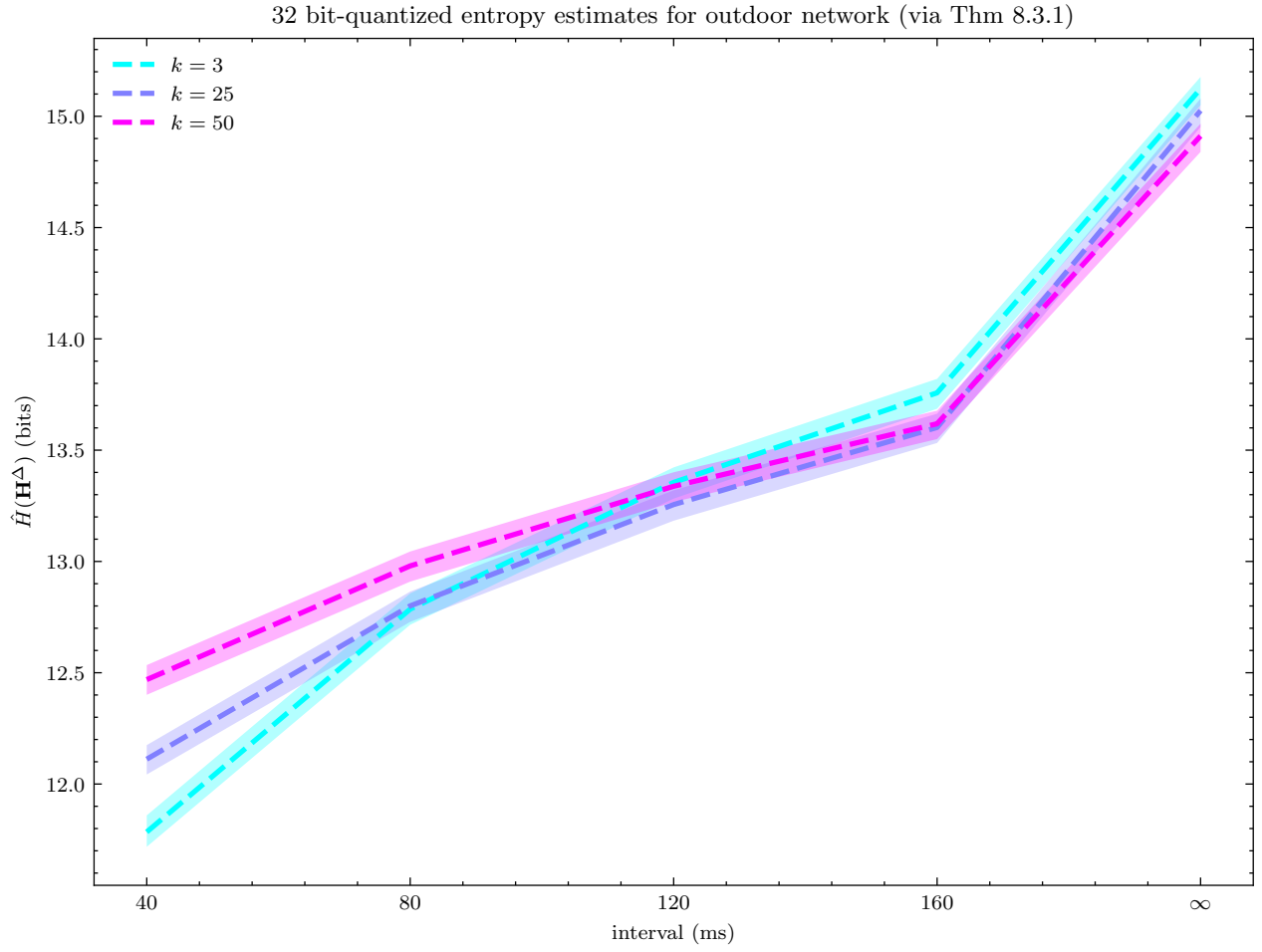

Figure: Mean entropy/conditional entropy estimates $\hat{H}(\mathbf{H}^{\Delta}) = \hat{h}(\mathbf{H}) + n$ with 95% c.i. for quantized i.i.d COST2100 elements vs. quantization level (bits).

Future Work: Rate-Distortion Bound

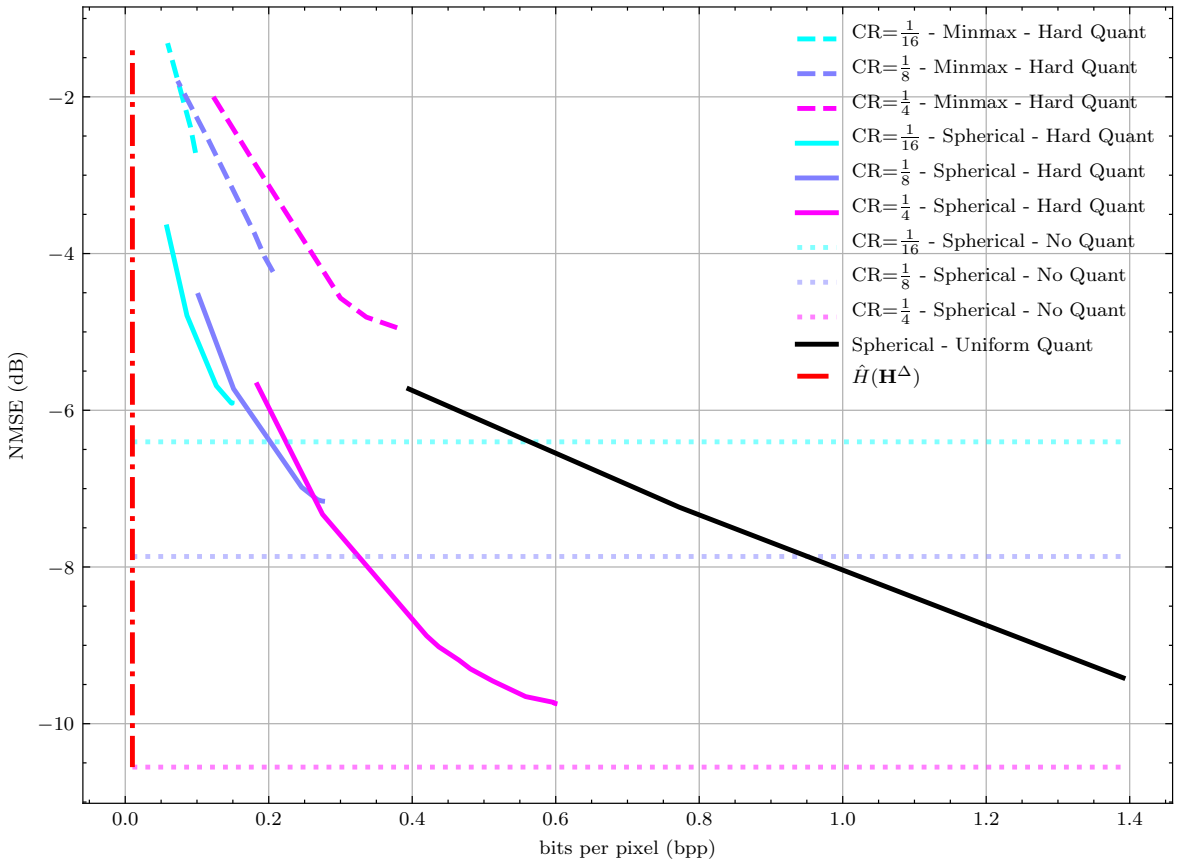

Figure: Rate distortion of CsiNet-SoftQuant on outdoor dataset with entropy bound based on differential entropy estimate.

Questions?

mdelrosa@ucdavis.edu

[1] E. Crespo Marques, N. Maciel, L. Naviner, H. Cai, and J. Yang, "A Review of Sparse Recovery Algorithms," *IEEE Access*, vol. 7, pp. 1300–1322, 2019.

[2] E. C. Marques, N. Maciel, L. A. B. Naviner, H. Cai, and J. Yang, "Compressed Sensing for Wideband HF Channel Estimation," in *2018 4th International Conference on Frontiers of Signal Processing (ICFSP)*, pp. 1–5, 2018.

[3] C. Wen, W. Shih, and S. Jin, "Deep Learning for Massive MIMO CSI Feedback," *IEEE Wireless Communications Letters*, vol. 7, pp. 748–751, Oct 2018.

[4] Z. Liu, **M. del Rosario**, X. Liang, L. Zhang, and Z. Ding, "Spherical Normalization for Learned Compressive Feedback in Massive MIMO CSI Acquisition," in *2020 IEEE International Conference on Communications Workshops (ICC Workshops)*, pp. 1–6, 2020.

[5] Z. Liu, L. Zhang, and Z. Ding, "Exploiting Bi-Directional Channel Reciprocity in Deep Learning for Low Rate Massive MIMO CSI Feedback," *IEEE Wireless Communications Letters*, vol. 8, no. 3, pp. 889–892, 2019.

[6] T. Wang, C. Wen, S. Jin, and G. Y. Li, "Deep Learning-Based CSI Feedback Approach for Time-Varying Massive MIMO Channels," *IEEE Wireless Comm. Letters*, vol. 8, pp. 416–419, April 2019.

[7] Z. Liu †, **M. del Rosario †**, and Z. Ding, "A Markovian Model-Driven Deep Learning Framework for Massive MIMO CSI Feedback," *arXiv e-prints*, Sept. 2020.

Submitted to IEEE Transactions on Wireless Communications.

[8] Q. Yang, M. B. Mashhadi, and D. Gündüz, "Deep Convolutional Compression For Massive MIMO CSI Feedback," in *2019 IEEE 29th International Workshop on Machine Learning for Signal Processing (MLSP)*, pp. 1–6, 2019.

[9] E. Agustsson, F. Mentzer, M. Tschannen, L. Cavigelli, R. Timofte, L. Benini, and L. Van Gool, "Soft-to-hard Vector Quantization for End-to-end Learning Compressible Representations," *Advances in Neural Information Processing Systems*, vol. 2017-Decem, no. NIPS, pp. 1142–1152, 2017.

[10] L. Kozachenko and N. N. Leonenko, "Sample Estimate of the Entropy of a Random Vector," *Problemy Peredachi Informatsii*, vol. 23, no. 2, pp. 9–16, 1987.

[11] T. M. Cover, *Elements of information theory*

Appendix

Multivariate Autoregression (MAR)

Rather than scalar $\hat{\gamma} \in \mathbb{R}^+$, we can derive a multivariate p-step predictor, $\mathbf{W}_1, \ldots, \mathbf{W}_p$. Given p prior CSI samples, the mean-square optimal predictor $\hat{H}_t$ is a linear combination of these the prior CSI samples,

$$\hat{\mathbf{H}}_t = \mathbf{H}_{t-1}\mathbf{W}_1 + \cdots + \mathbf{H}_{t-p}\mathbf{W}_p + \mathbf{E}_t. \tag{5}$$

Error terms are uncorrelated with the CSI samples (i.e. $\mathbf{H}_{t-i}^H \mathbf{E}_t = 0$ for all $i \in [0, \ldots, p]$), and we pre-multiply by $\mathbf{H}_{t-i}^H$,

$$\begin{aligned} \mathbf{H}_{t-i}^H \hat{\mathbf{H}}_t &= \mathbf{H}_{t-i}^H \mathbf{H}_{t-1} \mathbf{W}_1 + \cdots + \mathbf{H}_{t-i}^H \mathbf{H}_{t-p} \mathbf{W}_p + \mathbf{H}_{t-i}^H \mathbf{E}_t \\ &= \mathbf{H}_{t-i}^H \mathbf{H}_{t-1} \mathbf{W}_1 + \cdots + \mathbf{H}_{t-i}^H \mathbf{H}_{t-p} \mathbf{W}_p. \end{aligned} \tag{6}$$

Denote the correlation matrix $\mathbf{R}_i = \mathbb{E}[\mathbf{H}_{t-i}^H \mathbf{H}_t]$. We presume the CSI matrices are generated by a stationary process, and consequently, they have the following properties:

1. $\mathbf{R}_i = \mathbb{E}[\mathbf{H}_{t-i}^H \mathbf{H}_t] = \mathbb{E}[\mathbf{H}_t^H \mathbf{H}_{t+i}]$
2. $\mathbf{R}_i = \mathbf{R}_{-i}^H$

Taking the expectation, we can write (6) as a linear combination of correlation matrices,

$$\mathbf{R}_{i+1} = \mathbf{R}_i \mathbf{W}_1 + \cdots + \mathbf{R}_{i-p+1} \mathbf{W}_p.$$

For p CSI samples, we can write a system of p equations, which admits the following,

$$\begin{bmatrix} \mathbf{R}_1 \\ \mathbf{R}_2 \\ \dots \\ \mathbf{R}_p \end{bmatrix} = \begin{bmatrix} \mathbf{R}_0 & \mathbf{R}_1^H & \dots & \mathbf{R}_{p-1}^H \\ \mathbf{R}_1 & \mathbf{R}_0 & \dots & \mathbf{R}_{p-2}^H \\ \vdots & & \ddots & \vdots \\ \mathbf{R}_{p-1} & \mathbf{R}_{p-2} & \dots & \mathbf{R}_0 \end{bmatrix} \begin{bmatrix} \mathbf{W}_1 \\ \mathbf{W}_2 \\ \dots \\ \mathbf{W}_p \end{bmatrix}.$$

Solving for the coefficient matrices admits the solution

$$\begin{bmatrix} \mathbf{W}_1 \\ \mathbf{W}_2 \\ \dots \\ \mathbf{W}_p \end{bmatrix} = \begin{bmatrix} \mathbf{R}_0 & \mathbf{R}_1^H & \dots & \mathbf{R}_{p-1}^H \\ \mathbf{R}_1 & \mathbf{R}_0 & \dots & \mathbf{R}_{p-2}^H \\ \vdots & & \ddots & \vdots \\ \mathbf{R}_{p-1} & \mathbf{R}_{p-2} & \dots & \mathbf{R}_0 \end{bmatrix}^+ \begin{bmatrix} \mathbf{R}_1 \\ \mathbf{R}_2 \\ \dots \\ \mathbf{R}_p \end{bmatrix}, \tag{7}$$

where $[\cdot]^+$ denotes the Moore-Penrose pseudoinverse.

MarkovNet: Results ($\text{NMSE}_{\text{truncated}}$)

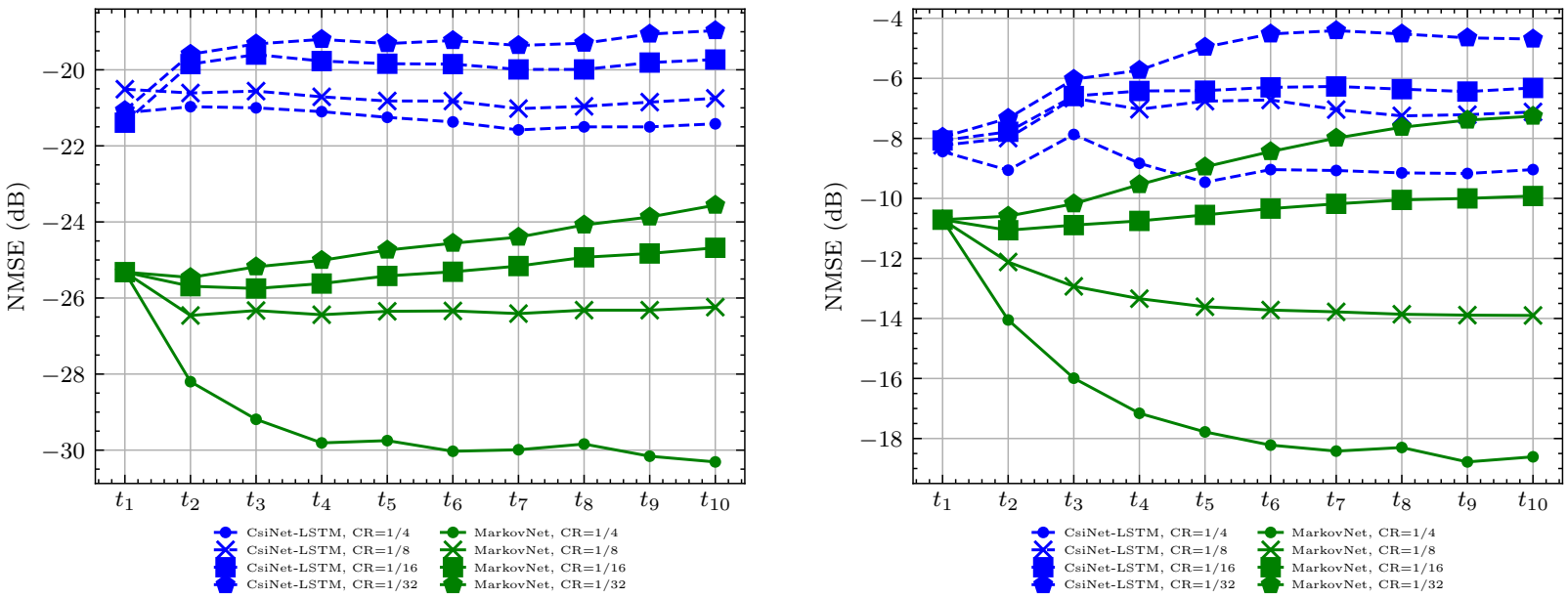

(a) Indoor (b) Outdoor

Figure: $\text{NMSE}_{\text{truncated}}$ comparison of MarkovNet and CsiNet-LSTM at various compression ratios (CR).

MarkovNet: Results (NMSE_{all})

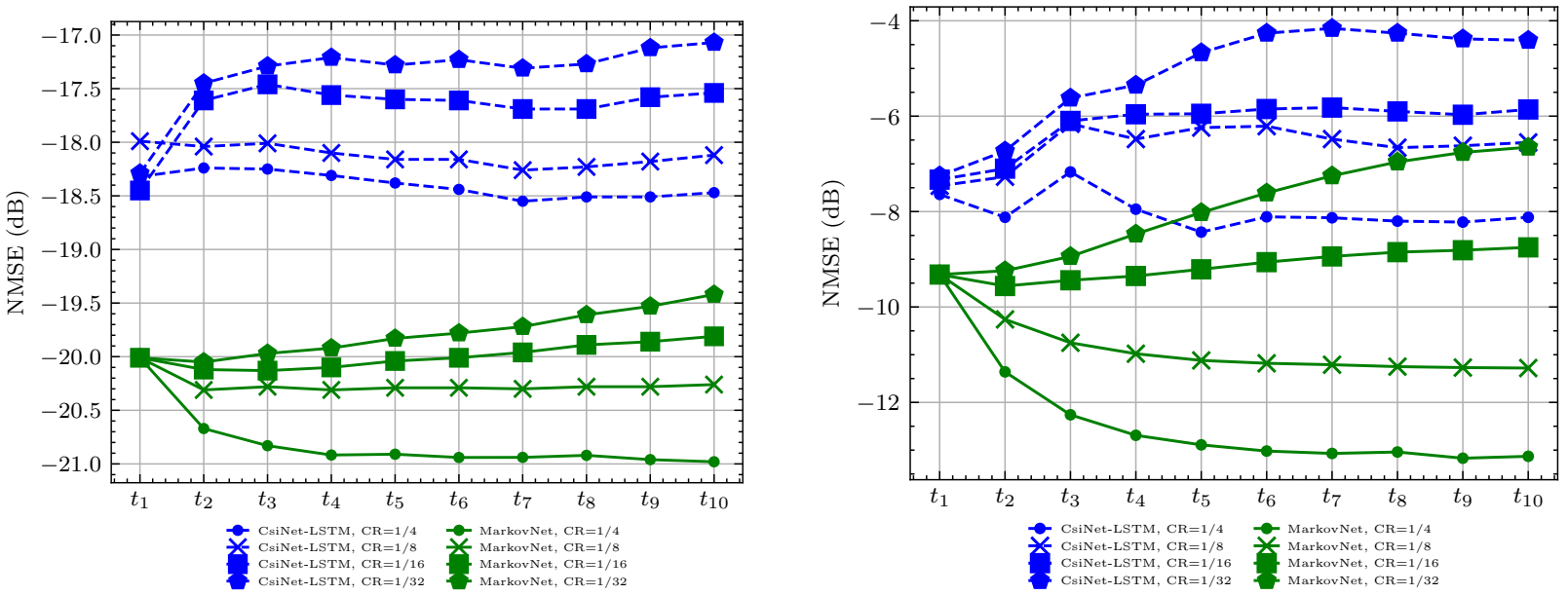

(a) Indoor (b) Outdoor

Figure: NMSE_{all} comparison of MarkovNet and CsiNet-LSTM at various compression ratios (CR).

Results: Rate-Distortion (Minmax, Soft vs. Hard)

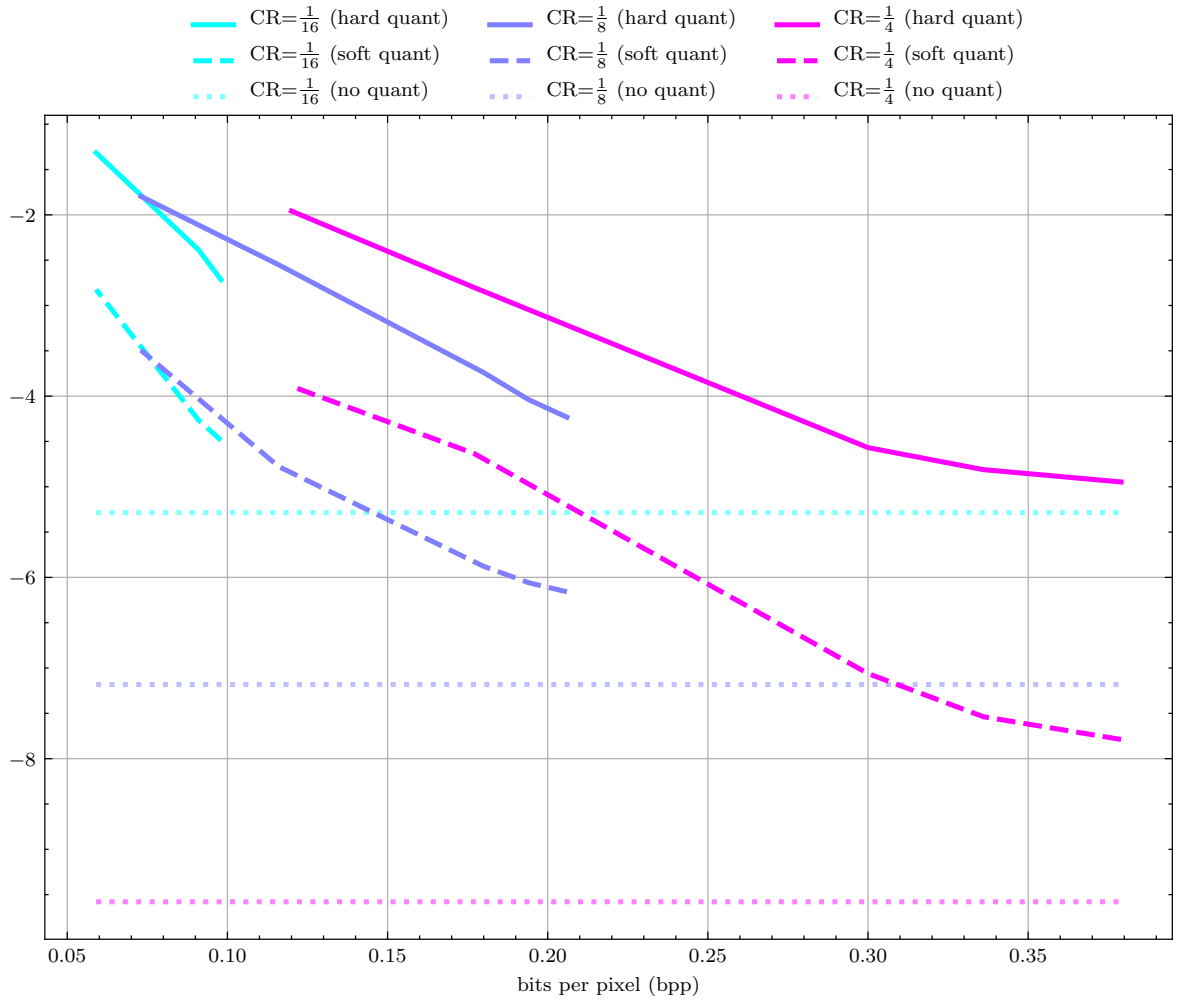

Figure: Rate distortion of CsiNet-SoftQuant under minmax normalization using: $L = 1024$ centers, $d = 4$.

Results: Rate-Distortion (Spherical, Soft vs. Hard)

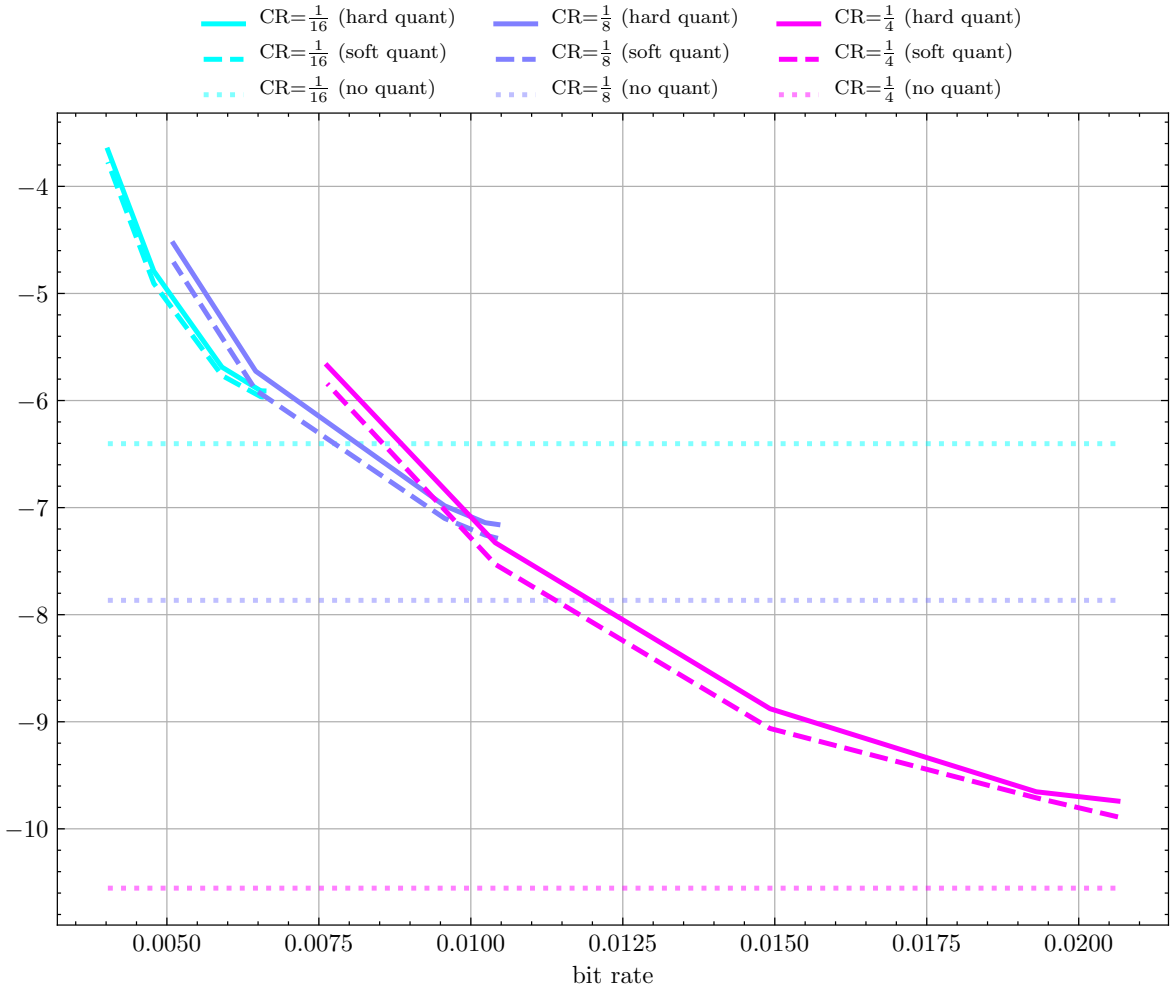

Figure: Rate distortion of CsiNet-SoftQuant using: $L = 1024$ centers, CR= $\frac{1}{4}$, $d = 4$. Bit rates are realized under arithmetic coding of quantized features.

Differential Entropy Estimation: Multivariate Normal

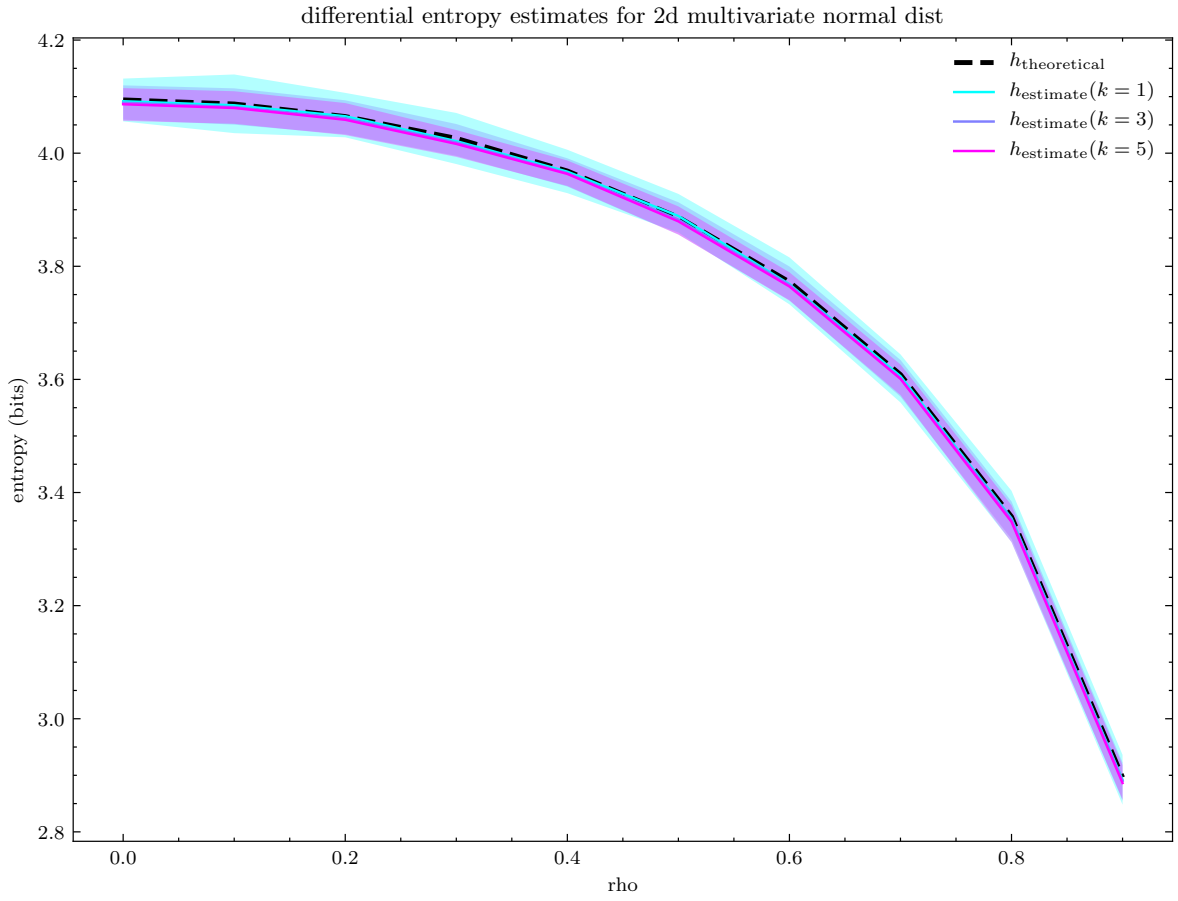

Figure: Differential entropy and estimates for 2d multivariate normal distribution. Estimates are based on the KL estimator [10] using the NPEET library [12].